

# Exploratory numerical experiments with a macroscopic theory of interfacial interactions

D. Giordano · P. Solano-López · J. M. Donoso

Received: date / Accepted: date

**Abstract** Phenomenological theories of interfacial interactions are founded on the core idea to model macroscopically the thin layer that forms between media in contact as a two-dimensional continuum (surface phase or interface) characterised by physical properties per unit area; the temporal evolution of the latter is governed by surface balance equations whose set acts as bridging channel in between the governing equations of the volume phases. These theories have targeted terrestrial applications since long time and their exploitation has inspired our research programme to build up, on the same core idea, a macroscopic theory of gas-surface interactions targeting the complex phenomenology of hypersonic reentry flows as alternative to standard methods in aerothermodynamics based on accommodation coefficients. The objective of this paper is the description of methods employed and results achieved in the exploratory study that kicked off our research programme, that is, the unsteady heat transfer between two solids in contact in planar and cylindrical configurations with and without interface. It is a simple numerical-demonstrator test case designed to facilitate quick numerical calculations but, at the same time, to bring forth already sufficiently meaningful aspects relevant to thermal protection due to the formation of the interface. The paper begins with a brief introduction on the subject matter and a review of relevant literature within an aerothermodynamics perspective. Then the case is considered in which the interface is absent. The importance of tension (force per unit area) continuity as boundary condition

on the same footing of heat-flux continuity is recognised and the role of the former in governing the establishment of the temperature-difference distribution over the separation surface is explicitly shown. Evidence is given that the standard temperature-continuity boundary condition is just a particular case. Subsequently the case in which the interface is formed between the solids is analysed. The coupling among the heat-transfer equations applicable in the solids and the balance equation for the surface thermodynamic energy more conveniently formulated in terms of the surface temperature is discussed. Results are illustrated and commented for planar and cylindrical configuration; they show unequivocally that the thermal-protection action of the interface turns out to be driven exclusively by thermophysical properties of the solids and of the interface; accommodation coefficients are not needed. Future work of more fluid-dynamics nature is mentioned in the concluding section.

**Keywords** Interfacial processes · Gas-surface interactions · Aerothermodynamics

## 1 Introduction

The physics housed inside the transition layer between two different media and the micro/macroscopic phenomena occurring therefrom have always attracted interest and attention of scientists concerned with a wide variety of applications across numerous departments of scientific knowledge. Historically, capillarity phenomena came first under scrutiny; since the times of Da Vinci, recognised [137, (note 1, page 551)] first investigator, they were studied thoroughly by reputed scientists of the calibre of Young [138], Laplace [79], Gauss [42], Poisson [106], Gibbs [43,44,45], Maxwell [84], van der Waals [135], Poincaré [105], Einstein [34] and Minkowski [87]. As usual, the natural blend of scientific

D. Giordano  
ESA - Estec, Keplerlaan 1, 2201 AZ Noordwijk, The Netherlands  
Tel.: +31 71 565 4392  
E-mail: Domenico.Giordano@esa.int

P. Solano-López, J. M. Donoso  
Dpt de Física Aplicada, ETSIAE, Universidad Politécnica de Madrid,  
Plaza Cardenal Cisneros 3, 29040 Madrid, Spain  
E-mail: Pablo.Solano@upm.es, Josemanuel.Donosos@upm.es

curiosity, necessities arising from new engineering applications, and improvements in experimental techniques kicked off and drove the evolution that, in the course of the years until nowadays, brought interest and attention to spread to and explore other sectors of the vast physical phenomenology in question. Impressive surveys, equipped with thorough collections of bibliographic references, are provided by Sagis [113] and Somorjai [130] with a view to terrestrial applications.

With the advent of the space age, aerothermodynamics (ATD) joined the collection of engineering applications for which the media-in-contact phenomenology assumes a role, and a rather crucial one in this case. In ATD parlance, the term *gas-surface interactions* (GSI) identifies the complex phenomenology of physical processes that occur inside the extremely thin transition layer between hypersonic flows in thermo-chemical nonequilibrium and the walls of either a spacecraft during planetary (re)entry or a test probe in high-enthalpy wind tunnels. These physical processes produce macroscopically the *superficial* exchange and transport of mass, momentum, energy and play a key role for the determination of several physical-variable distributions in both volume phases (fluid and solid) that turn out to be of utmost importance for heat-shield design. Among those physical variables, the wall heat flux is undoubtedly the most critical to aerothermodynamicists' concern.

The theoretical understanding and physical as well as numerical modeling of the superficial processes is essential for establishment and exploitation of the correct boundary conditions necessary for the (numerical) solution of the field equations governing the volume phases. Since the dawn of ATD, the GSI phenomenology has been approached in empirical manners, seemingly different in level of sophistication, that attempt to characterise the workings of the superficial processes by *accommodation coefficients* (ACs), whose conceptual introduction is claimed to Knudsen [63] by Goodman and Wachman [49] or to Langmuir [78] by Billing [22] and Zangwill [139], and by-product parameters derived therefrom. Study, development and application of AC-structured models [4, 9, 10, 11, 16, 33, 38, 40, 58, 64, 66, 67, 68, 71, 72, 74, 75, 94, 95, 99, 103, 114, 118, 119, 131, 134] have proliferated in the course the 60 years elapsed from the appearance of the pioneering papers by Lees [80], Fay and Riddell [37], Probst [107] and Goulard [50]; the process is still ongoing nowadays. We refer readers wishing to acquire deeper familiarity with the subject matter to the thorough surveys of methods and literature provided by Kovalev and Kolesnikov [74] and Viviani [133]. Although there are attempts [26, 27, 30, 111, 112, 140] to determine ACs from quantum-mechanical, molecular-dynamics (MD) and Monte-Carlo calculations, efforts and energies (financial form included) have been invested prevalently in experimental investigations [6, 7, 8, 15, 35, 54, 58, 65, 69, 70, 72, 82, 83, 100, 101, 102, 104, 117].

As a matter of consequence, empirical GSI models incorporate implicitly experimental information, confidently accurate for sure from the standpoint of experimental-testing art but of unexplored and therefore questionable physical significance, to provide *realistic* (?) numbers for ACs and related variables. Indeed, and experimental imprimatur notwithstanding, there is still a broad variety of opinions among aerothermodynamicists regarding the correct and, above all, *convincing* answer to a several-decade old but still lingering question: what *independent* physical variables do the ACs depend on? Collectable answers from workers in the field are manifold and, regrettably, contradictory. After almost three decades (in Europe) of AC practice and operations, it seems (to us) fair to admit that the theoretical/numerical state of the AC art is today still rather far away from deserving satisfactory engineering confidence. The main reason for the virtual distance to the latter target lies in the true nature of the AC-concept: it is a heuristic, empirical construct lacking support from an underlying rigorous and self-contained physical theory, as explicitly declared also by Kovalev and Kolesnikov [74]. Broadly speaking, ACs and derived by-products are nothing more than empirical parameters whose usage is a kind of numerical subterfuge to avoid paying attention to the complex details of the physical processes going on inside the transition layer. AC methodologies are habitually trusted with owning predictive power and capabilities to shortcut, or even elude, superficial-process complexities, presumptively conferred on them without perhaps realising the great risk lurking behind that conferral: the in-vain tentative to describe in an *algebraic* manner a physical phenomenology that is governed by differential equations whose boundary conditions' variety pulverises any however perceptibly small allusion to the existence of algebraic functions for the ACs. In our opinion, the AC-modeling pathway is conceptually unsatisfactory, inherently difficult and rather uncontrollable as far as accuracy is concerned, mainly because experimental testing with high-temperature flows in thermochemical non-equilibrium is costly and not as thoroughly feasible as one would wish for the purpose of explaining through the AC-modeling pathway all the open question marks of the GSI phenomenology; as a result, prediction reliability and engineering effectiveness of AC-based empirical GSI models could be severely compromised.

After slightly more or less than *one century* since Knudsen [63] and/or Langmuir [78] proposed the AC concept and with ATD applications in mind, it appears (to us) unavoidable to confront an obvious, and maybe hopeless, question: will any major breakthrough be ever achieved by obstinate persistence on the AC-modeling pathway? The majority of aerothermodynamicists has resigned to persistence and endures case-by-case engineering challenges, and perhaps justifiably so because *at the moment* there is no other alternative compatible with the rigid time frames imposed by heat-

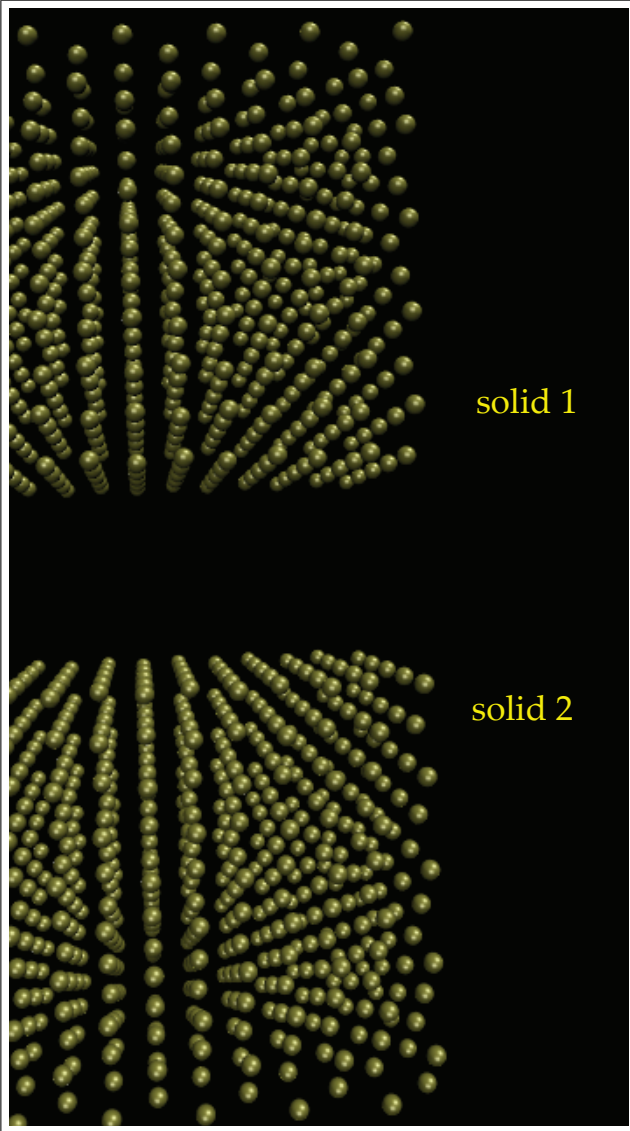


**Fig. 1** Microscopic view of two blocks of platinum in contact at a distance of 4 ångströms. Courtesy of Prof S V Nedeä, dpt of Mechanical Engineering, Technical University of Eindhoven

shield design. However, a few of them, lucky enough to be unconstrained by design necessities, believe time is mature to, at least, explore other scientific avenues.

## 2 Theoretical considerations

The correct mathematical description of interfacial physics presupposes a clear understanding of what happens at microscopic level [2, 22, 49, 51, 89, 129, 139] in the transition layer. As simple and convenient entry point into the discourse, let us consider two stationary solids in contact as sketched in Fig. 1. Obviously, the *contact* concept is macroscopic in nature because the atoms in the terminal rows of the solids do not really *touch*; they stand off at a minute dis-

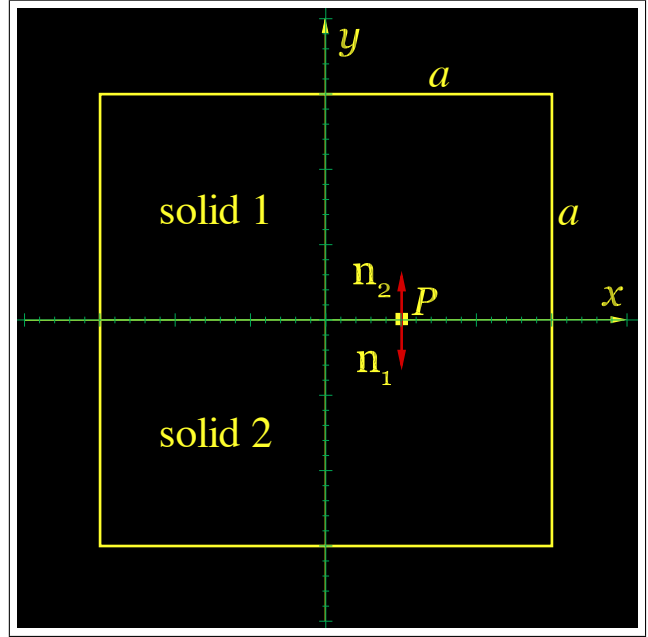


**Fig. 2** Macroscopic representation of the platinum contact sketched in Fig. 1

tance established by the interplay between the forces due to the repulsive potential that comes to exist in the region where the terminal rows are facing each other and other external forces imposed on the solids. Exchanges of momentum and energy between the solids occur through the mediating action of the potential, unconditionally modelled as action-at-distance-like (for simplicity, let us imagine also radiation negligible and put it aside). It appears evident that, under this circumstance, momentum and energy leaving one solid per unit area in the unit time can only go into the other solid. Thus, the thermodynamic-energy exchange in heat-transfer problems is consistently subjected macroscopically (Fig. 2) to heat-flux continuity

$$\mathbf{n}_1 \cdot \mathbf{J}_{U,1}(P, t) + \mathbf{n}_2 \cdot \mathbf{J}_{U,2}(P, t) = 0 \quad (1)$$

in any instant of time  $t$ . Equation (1) is a straightforward consequence of the principle of total-energy conservation, although only the thermodynamic form  $U$  is at play in this case. However, heat-flux continuity alone is not sufficient to describe the heat-transfer dynamics. Another physical condition is needed and temperature continuity

$$T_1(P, t) - T_2(P, t) = 0 \quad (2)$$

(or even its more sophisticated contact-resistance version) turns out to be customarily enforced. Equation (2) is a typical example of intuitively imposed *ad-hoc* condition. Indeed, although a widely exploited textbook standard [29, 55], Eq. (2) becomes conceptually a bit problematic when the underlying justifying physical principle is sought for. In fact, there is none. Sometimes vague claims appealing to

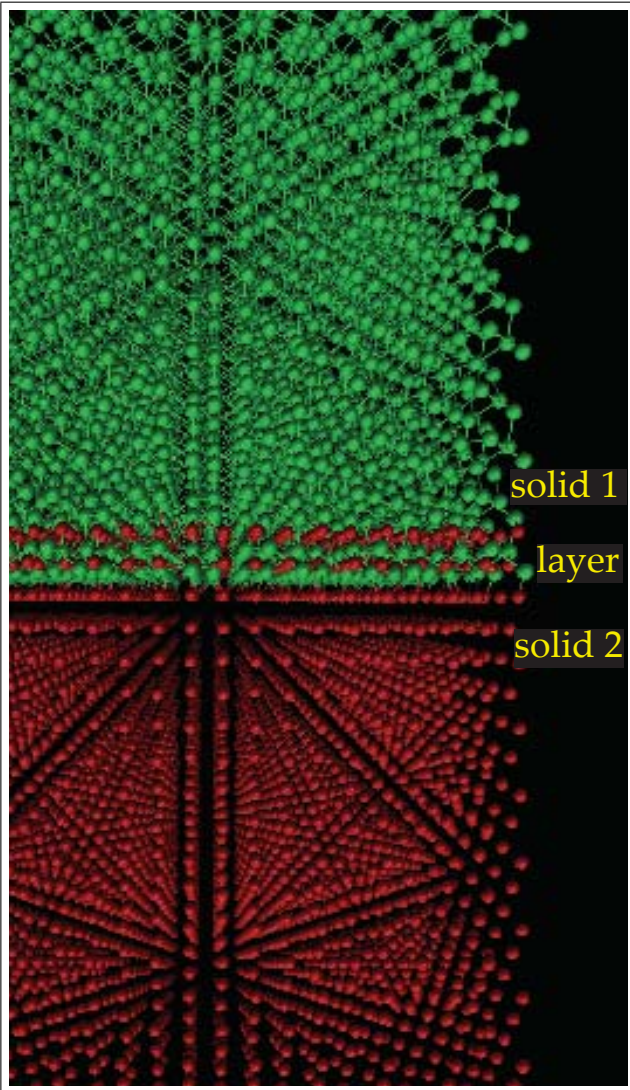


**Fig. 3** Microscopic view of a block of silicon (solid 1) and a block of platinum (solid 2) separated by a thin mixed layer. Courtesy of Prof S V Nedeia, dpt of Mechanical Engineering, Technical University of Eindhoven

(typically unreferenced) experimental evidence are invoked to support the unconditional enforcement of Eq. (2) but they are easily contrasted and dismissed by documented experimental evidence showing the opposite as, for example, the results reported by Fang and Ward [36] for a liquid-vapour interface. We will come back to this interesting aspect in the sequel (Sec. 3).

If the external forces are sufficiently intense, the microscopic situation turns into the one sketched in Fig. 3: the terminal rows of atoms compenentrate and form a thin layer of microscopic thickness that cannot be considered either solid 1 or solid 2. Physical properties leaving one solid per unit area in the unit time do not go directly into the other solid but have to cross the thin layer first, and it is clear that, therein, they can be locally accumulated, produced, and, rather inter-

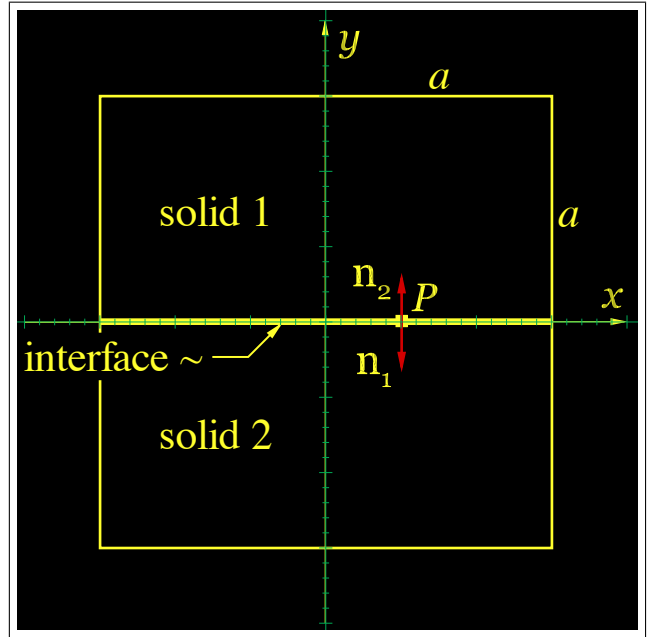


**Fig. 4** Macroscopic representation of the silicon-platinum contact sketched in Fig. 3; planar interface.

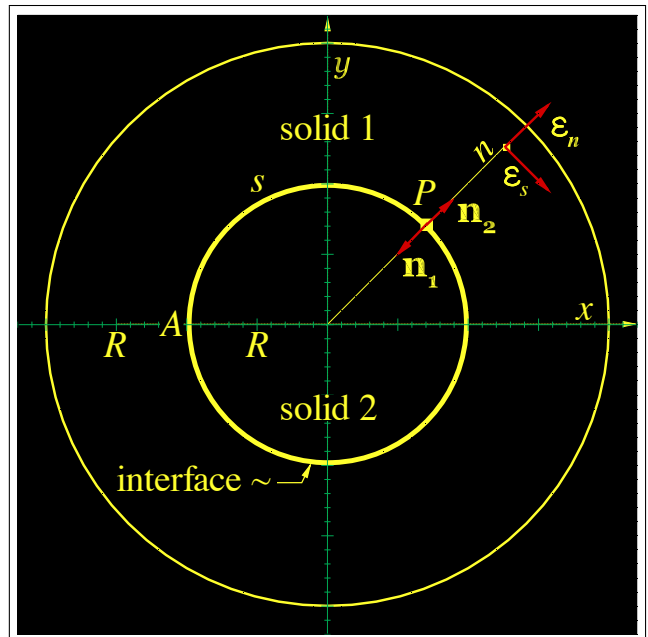


**Fig. 5** Macroscopic representation of two-solid cylindrical contact; curved interface.

estingly, *tangentially* transported, by diffusion in this case. In other words, the thin layer that forms between the media in contact turns out to be a third medium with its own physical properties (mass, momentum, energy in its various forms and total, etc) that follow their own evolutionary dynamics. With this microscopic picture in mind, the foundational idea on which a phenomenological theory can be built is to model the thin layer macroscopically as a *two-*

dimensional continuum, a *surface phase* or *interface* in between the volume phases, characterised by physical properties per unit area. Since Gibbs introduced the embryonic form of this idea in his seminal memoirs [43,44,45], also included in his collected works [46,47], within a thermodynamics context limited to energy and entropy, it has been pursued, explored and made evolve during the course of the years again in thermodynamics [25,31,41,52,88,91,97,115] as well as in kinetic theory (KT) [23,24,76,77], linear irreversible thermodynamics (LIT) [3,13,14,62,41,73,91,98,113,136], and phenomenological theory [32,41,48,53,56,57,81,92,93,108,109,110,113,120,126,127,128]; familiarisation with the mentioned literature, and that contained therein, is indispensable for those who wish to endeavour to work in this scientific domain.

The evolution of the superficial physical properties is governed by superficial balance equations that play a bridging role between the field equations governing the evolution of the physical properties belonging to the volume phases. The three sets of equations are obviously coupled and require a simultaneous (numerical) solution. We recommend readers interested in specific details and rigorous mathematical derivations to consult the mentioned literature, in particular Bedeaux et alii [13,14], Gatignol and Prud'homme [41], Gogosov et alii [48], Napolitano [91,92,93], Slattery [126,127], and Slattery et alii [128]; our notation and terminology will follow very closely those adopted by Napolitano. The mathematical structure of the superficial balance equations is conceptually very similar to the familiar one of the balance equations applicable in the volume phases; the formal one corresponding to the generic scalar or vectorial extensive physical variable  $G$  reads

$$\frac{\partial \tilde{g}}{\partial t} + \nabla_s \cdot [\tilde{\mathbf{v}}\tilde{g} - \mathbf{n} \times (\mathbf{n} \times \tilde{\mathbf{J}}_G)] = \mathbf{n}_1 \cdot \tilde{\Phi}_{G,1} + \mathbf{n}_2 \cdot \tilde{\Phi}_{G,2} + \dot{\tilde{g}} \quad (3)$$

In Eq. (3),

$\tilde{g}$	superficial density
$\nabla_s$	surface-gradient operator
$\tilde{\mathbf{v}}$	superficial mass velocity
$\mathbf{n}_k$	surface-normal unit vector for volume phase $k$ ( $=1,2$ ); chosen outwards by convention
$\mathbf{n}$	surface-normal unit vector (either of the two)
$\tilde{\mathbf{J}}_G$	superficial diffusive flux
$\tilde{\Phi}_{G,k}$	total flux in volume phase $k$
$\dot{\tilde{g}}$	superficial production

Equation (3) applies locally in each geometrical point of the interface. The term

$$\mathbf{n}_1 \cdot \tilde{\Phi}_{G,1} + \mathbf{n}_2 \cdot \tilde{\Phi}_{G,2} \quad (4)$$

on the right-hand side is the total-flux jump across the interface and represents the main, although not the only one, channel of physical-property exchange between the interface and the volume phases. The total flux in volume phase

$k$  is obviously separable in convective and diffusive contributions

$$\tilde{\Phi}_{G,k} = \rho_k (\mathbf{v}_k - \mathbf{w}) g_k + \mathbf{J}_{G,k} \quad (5)$$

with

$\rho_k$	mass density
$\mathbf{v}_k$	mass velocity
$\mathbf{w}$	interface <i>geometrical</i> velocity
$g_k$	volume density
$\mathbf{J}_{G,k}$	diffusive flux

Of course, the superficial balance equations [Eq. (3)] are in open form and require to be complemented with phenomenological relations for superficial diffusive fluxes and productions, exactly as it happens for the volume-phase balance equations. The phenomenological relations are expected to be provided by joint efforts and combined contributions from MD, thermodynamics, LIT, and KT *of the interface*, desirably supported by experimental verification, if any be possible. In this regard, there is a noticeable volume of knowledge already available in the literature mentioned in the two paragraphs above Eq. (3). The concept of *two-dimensional fluid dynamics* may sound exotic to some of us but this intuitive (perhaps even emotional sometimes) reaction is just a consequence of mental habit acquired in years, educational and professional, of dealing and practicing with applications in three-dimensional space behaving marvelously well according to the Euclidean prescript. The habit buildup starts early in our formation days: in general, fluid-dynamics textbooks default, without deliberate and explicit recognition, to such a spatial circumstance and unravel physical concepts in mathematical formalisms framed on systems of orthogonal coordinates among which the Cartesian ones are particularly more privileged than the curvilinear ones. There is a laudable exception though: Sedov [121,122,123,124] teaches continuum mechanics in Riemann space and uses co/contravariant non-orthogonal curvilinear coordinates throughout (a really mind-broadening learning experience!). An additional setback is the absence of two-dimensional fluid dynamics in universities' syllabuses and the systematic lack of consideration for it in textbooks. But also in this regard there is a commendable exception: Aris [5], after preliminarily introducing "the geometry of surfaces in space" (chapter 9), provides an interesting treatment of "the equations of surface flow" (chapter 10) admittedly inspired and based on Scriven's work [120]. In the paragraph introducing the latter chapter, he emphasises straight off two among the most important and crucial characteristics of interfaces. The first:

... Cartesian tensors really suffice for three-dimensional flows; for the space of everyday life, being Euclidean, always admits of a Cartesian frame of reference. However, the surface is a two-dimensional



non-Euclidean space and from the outset demands a full tensorial treatment.

This characteristic follows by necessity from the fact that the

... surface is a two-dimensional space that can move within a space of higher dimensions, namely, the three-dimensional space surrounding it.

Thus, position and shape of the interface are, in general, time dependent and not known *a priori*; in other words, the geometrical equation of the interface

$$\mathbf{r}_s = \mathbf{r}_s(\xi_1, \xi_2, t) \quad (6)$$

is an unknown of the problem and, consequently, the Gaussian curvilinear coordinates  $(\xi_1, \xi_2)$  cannot be assumed unconditionally orthogonal from the outset. The necessity of a full tensorial treatment is so essential that Napolitano [90] dedicated a full paper and Gatignol and Prud'homme [41] a thorough appendix to the subject matter although, peculiarly enough, these authors target only orthogonal curvilinear coordinates. Incidentally, the motion of the interface affects explicitly the fluxes [Eq. (5)] through the presence of the geometrical velocity defined as

$$\mathbf{w} = \left( \frac{\partial \mathbf{r}_s}{\partial t} \right)_{\xi_1, \xi_2} \quad (7)$$

The second characteristic

... [the interface] may be the region of contact of two bulk fluids. This is again a new feature, for a bulk fluid can never be the interface of two four-dimensional fluids.

follows from the presence of the total-flux jump [Eq. (4)], a property belonging to the volume phases, in the superficial balance equations [Eq. (3)]. It is the element that appoints the superficial balance equations to the role of boundary conditions, an aspect specifically discussed in Sec. 10.51 ("Surface equations as boundary conditions at an interface"), also prototyped by Waldmann [136] and repeatedly stressed by Bedeaux et alii [13, 14] and Napolitano [91, 92, 93]. In this regard, we should not miss an essential point already mentioned in Sec. 1: the physical-property exchanges through the interface constitute a physical phenomenology governed by differential equations [Eq. (3)] and any attempt to describe it algebraically, as done along the AC-modeling pathway, is hopelessly ill-fated.

In conclusion, it should appear evident from the previous considerations that a phenomenological theory of interfaces targeting non-space applications has been maturing since long time. The novelty of our research program is the tentative extension of such a phenomenological theory to build a branch, a macroscopic theory of gas-surface

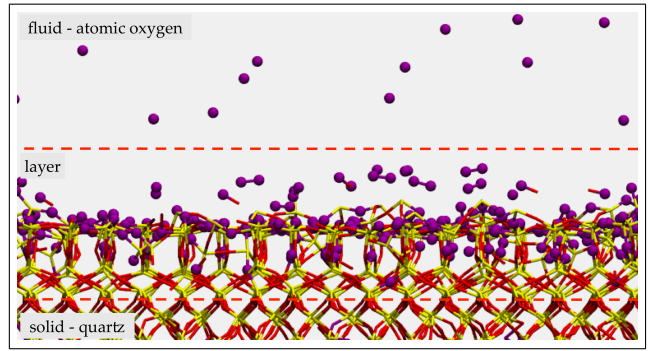


**Fig. 6** Microscopic view of DSMC-reconstructed quartz surface exposed to atomic oxygen. Courtesy of Prof T Schwartzentruber, dpt of Aerospace Engineering and Mechanics, University of Minneapolis

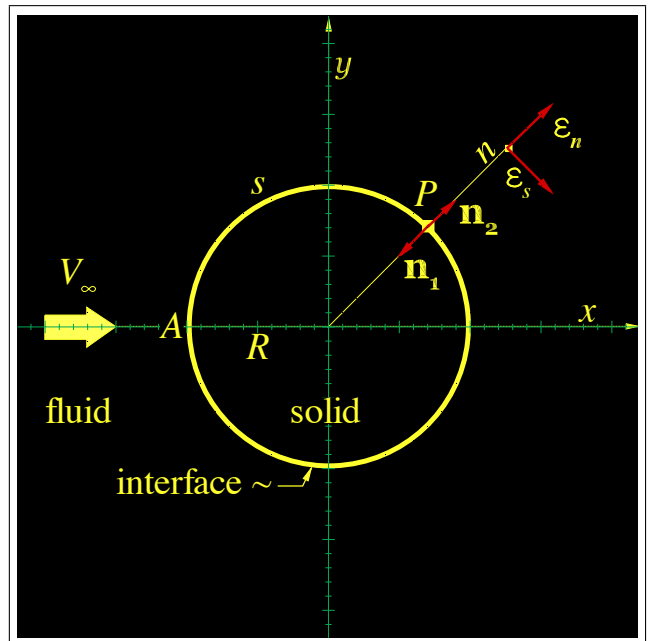


**Fig. 7** Future study: two-dimensional flow past a cylinder with (and without) interface.

interactions (MTGSI), targeting the complex phenomenology featured by hypersonic reentry flows as alternative to the AC-modeling pathway. Clearly, the idea of interface formation, and its macroscopic modelling as a two-dimensional continuum, can be smoothly exported without any particular conceptual difficulty to the case of fluid-solid contact; examples of microscopic view and a possible macroscopic configuration are sketched in Figs. 6 and 7. Nevertheless, the achievement of the preparedness to deal theoretically, mathematically and numerically with the global set of coupled governing equations for fluid, solid and interface appears a rather ambitious feat at this stage of our research programme. This sensation becomes even more acute in view of confronting the very complex physical phenomenology embraced by aerothermodynamics. The phenomenological-relation know-how acquired for non-space problems [see

bibliographic references mentioned before Eq. (3)] will certainly require further advancement to shed light on and to bring within reach the complexities of not only familiar, although still ill-understood, processes such as superficial chemical kinetics and ablation but also of others playing a role in Eq. (3) and ignored right now because they are invisible along the AC- and ablation-modeling pathways. As explicit example, and a rather significant one by the way, let us scrutinise the balance

$$\begin{aligned} \frac{\partial \tilde{\rho}_i}{\partial t} + \nabla_s \cdot [\tilde{\rho}_i \tilde{\mathbf{v}} - \mathbf{n} \times (\mathbf{n} \times \tilde{\mathbf{J}}_i)] = \\ \mathbf{n}_1 \cdot [\rho_{i,1}(\mathbf{v}_1 - \mathbf{w}) + \underline{\mathbf{J}}_{i,1}] \\ + \mathbf{n}_2 \cdot [\rho_{i,2}(\mathbf{v}_2 - \mathbf{w}) + \underline{\mathbf{J}}_{i,2}] \\ + \sum_r \underline{\tilde{\xi}}_r \underline{\mathbf{v}}_{ri} M_i \end{aligned} \quad (8)$$

of the superficial mass of a chemical component. In Eq. (8), the subscripts  $i$  and  $r$  point respectively to chemical component and chemical reaction, and

$\tilde{\rho}_i$	superficial partial density
$\tilde{\mathbf{J}}_i$	superficial-mass diffusive flux
$\rho_{i,k}$	volume-phase partial density ( $k = 1$ is gas, $k = 2$ is solid)
$\underline{\mathbf{J}}_{i,k}$	volume-phase mass diffusive flux
$\underline{\tilde{\xi}}_r$	superficial chemical-reaction rate
$\mathbf{v}_{ri}$	stoichiometric coefficient
$M_i$	molecular mass

AC-structured models shut convective fluxes and solid-side diffusive flux on the right-hand side of Eq. (8) out of the picture and contemplate exclusively the interplay between the underlined terms that describe, respectively, gas-side mass diffusion, systematically assumed governed by the poorly-performing Fick law, and superficial chemical kinetics; in turn, ablation models [17, 18, 19, 20, 21, 59, 60, 61, 86, 132] allow the convective fluxes to operate. In so doing, those models disregard mass diffusion in solids, which is not an unknown phenomenology [1, 12, 39, 85, 125], and, more importantly, miss the full extent of role played and consequences produced by the terms appearing on the left-hand side of Eq. (8), particularly those that bring into account convective ( $\tilde{\rho}_i \tilde{\mathbf{v}}$ ) and diffusive ( $\tilde{\mathbf{J}}_i$ ) transport *tangentially within* the interface. With specific regard to AC-structured models, there is no amount of squeezing *algebraic* coefficients into the expressions of the superficial chemical-reaction rates ( $\underline{\tilde{\xi}}_r$ ) that will substitute for the left-hand-side terms and will establish physical equivalence with and prediction capability of the full *differential* equation.

The previous example provides sufficient hints of the broader scope of the MTGSI-modeling pathway and also of the conceptual hurdles disseminated along it; we need not

to delve further into the meanders of the superficial balance equations of other physical properties such as total mass, momentum, etc., to convince ourselves that the list of conceptual corners awaiting illumination and exploration is obviously rather long. We wish, of course, to undertake the self-learning exploration walk-through in steps of increasing difficulty. As start-up of our research program, therefore, we concentrate on the exploratory study of the heat-transfer test case mentioned in the beginning of this section in planar and cylindrical configurations with and without interface. It should be looked at as a numerical demonstrator, simple enough to allow quick numerical computations but already sufficiently meaningful to bring forth important aspects relevant to thermal protection arising from the presence of an interface; to some extent, it also brings to completion the work initiated by Schmidtman [116]. As by-product, we show that, under circumstances of interface absence as sketched in Fig. 1, the popular temperature-continuity boundary condition [Eq. (2)] turns out to be a particular case whose customarily assumed unconditional applicability is not justified by any physical principle of conservation.

### 3 Heat-transfer test case without interface

#### 3.1 Theoretical considerations

In the case of absent interface ( $\tilde{g} \rightarrow 0, \tilde{\mathbf{J}}_G \rightarrow 0$ ), the surface balance equation [Eq. (3)] for a conservative ( $\dot{g} = 0$ ) variable  $G$  reduces to the familiar total-flux jump condition

$$\mathbf{n}_1 \cdot \underline{\Phi}_{G,1} + \mathbf{n}_2 \cdot \underline{\Phi}_{G,2} = 0 \quad (9)$$

that, for solids as those of Fig. 1 for example ( $\mathbf{v}_k = \mathbf{w} = 0$ ), simplifies even further to involve only the diffusive fluxes

$$\mathbf{n}_1 \cdot \underline{\mathbf{J}}_{G,1} + \mathbf{n}_2 \cdot \underline{\mathbf{J}}_{G,2} = 0 \quad (10)$$

The specialisation of Eq. (10) to total mass ( $G = m$ ) is identically satisfied because total mass cannot diffuse ( $\underline{\mathbf{J}}_{m,k} = 0$ ) by definition. The specialisation of Eq. (10) to thermodynamic energy ( $G = U$ ) reproduces the heat-flux continuity [Eq. (1)] that we have already considered in Sec. 1. The specialisation of Eq. (10) to momentum ( $G = \mathbf{Q}$ ) leads to tension (force per unit area) continuity

$$\mathbf{n}_1 \cdot \underline{\boldsymbol{\tau}}_1 + \mathbf{n}_2 \cdot \underline{\boldsymbol{\tau}}_2 = 0 \quad (11)$$

In Eq. (11),  $\underline{\boldsymbol{\tau}}_k = -\underline{\mathbf{J}}_{\mathbf{Q},k}$  is the stress tensor in solid  $k$ . If we take into account that stresses in solids depend on local temperature [28, 55] then we understand right away that Eq. (11) contains and provides the other condition that, together with heat-flux continuity [Eq. (1)], governs the establishment of the temperature difference  $T_1(P, t) - T_2(P, t)$

(Fig. 2); thus, the *physical* tension-continuity condition gently relegates the *intuitive* temperature-continuity condition [Eq. (2)] to the role of particular case.

In order to make these theoretical considerations explicit with simple test cases, and for the purpose of easiness in numerical calculations, we assume the solids to be isotropic, to follow Fourier law

$$\mathbf{J}_{U,k} = -\lambda_k \nabla T_k \quad (12)$$

and to feature a tensional behaviour described by Hooke law with linearised thermal-stress contribution [55]

$$\boldsymbol{\tau}_k = \boldsymbol{\tau}_{e,k} - \beta_k (T_k - T_{0,k}) \mathbf{U} \simeq -\beta_k (T_k - T_{0,k}) \mathbf{U} \quad (13)$$

In Eqs. (12) and (13)

$\lambda_k$	thermal conductivity in solid $k$ ( $=1,2$ )
$\nabla$	volume-gradient operator
$\boldsymbol{\tau}_{e,k}$	stress-tensor elastic part
$\beta_k$	thermal-stress coefficient [28]
$T_{0,k}$	reference temperature
$\mathbf{U}$	unit tensor

The thermal-stress coefficients can be expressed as

$$\beta_k = \frac{E_k}{1 - 2\nu_k} \alpha_k \quad (14)$$

In Eq. (14)

$E_k$	Young modulus
$\nu_k$	Poisson ratio
$\alpha_k$	linear thermal-expansion coefficient [55] or thermal-strain coefficient [28]

Thermodynamic and transport properties are scalar as a consequence of the isotropy of the solids and are assumed constant for simplicity. In Eq. (13), we consider negligible the stress-tensor elastic part with respect to the thermal-stress contribution for the simple reason of avoiding to consider deformations in the solids. The inclusion of stress-tensor elastic part and deformation field is, of course, doable but introduces the numerical complicacy of solving the deformation field together with the temperature field, an unnecessary sophistication in the context of the present discourse and that, by itself, does not add or remove any physical significance to the numerical results described in the following sections.

On the basis of the previous set of assumptions, Eq. (1) particularises to

$$\lambda_1 \mathbf{n}_1 \cdot \nabla T_1|_{P,t} + \lambda_2 \mathbf{n}_2 \cdot \nabla T_2|_{P,t} = 0 \quad (15)$$

and Eq. (11) reduces to a vector equation only in the normal direction ( $\mathbf{n}_k \cdot \mathbf{U} = \mathbf{n}_k$ )

$$\beta_1 [T_1(P,t) - T_{0,1}] \mathbf{n}_1 + \beta_2 [T_2(P,t) - T_{0,2}] \mathbf{n}_2 \simeq 0 \quad (16)$$

from which we obtain the scalar condition ( $\mathbf{n}_2 = -\mathbf{n}_1$ )

$$\beta_1 [T_1(P,t) - T_{0,1}] - \beta_2 [T_2(P,t) - T_{0,2}] \simeq 0 \quad (17)$$

enforcing tension continuity in the normal direction. Temperature continuity is recovered in the particular case when  $\beta_1 = \beta_2$  and  $T_{0,1} = T_{0,2}$ .

### 3.2 Application to planar configuration

With reference to Fig. 2, we assume

- adiabatic vertical walls

$$\left( \frac{\partial T_k}{\partial x} \right)_{x=\pm a} = \left( \frac{\partial T_k}{\partial z} \right)_{z=\pm a} = 0 \quad (18)$$

- uniform initial temperature

$$T_k(x, y, z, 0) = T^i \quad (19)$$

- uniform temperature at the top of solid 1 increasing linearly in time, within a finite interval  $\mathbb{T}$ , from the initial value  $T^i$  to a final value  $T^f$

$$T_1(x, +a, z, t) = \begin{cases} T^i & t < 0 \\ T^i + (T^f - T^i) \frac{t}{\mathbb{T}} & 0 \leq t \leq \mathbb{T} \\ T^f & \mathbb{T} < t \end{cases} \quad (20)$$

- uniform temperature at the bottom of solid 2 kept at the initial value

$$T_2(x, -a, z, t) = T^i \quad (21)$$

This set of boundary conditions [Eqs. (18)–(21)] determines a one-dimensional unsteady heat transfer in the  $y$  direction governed by the standard diffusion equation

$$\rho_k c_k \frac{\partial T_k}{\partial t} = \lambda_k \frac{\partial^2 T_k}{\partial y^2} \quad (22)$$

In Eq. (22)

$\rho_k$	density of solid $k$ ( $=1,2$ )
$c_k$	specific heat

The boundary conditions at the separation surface [Eqs. (15) and (17)] become

$$\lambda_1 \left( \frac{\partial T_1}{\partial y} \right)_{y=0^+} - \lambda_2 \left( \frac{\partial T_2}{\partial y} \right)_{y=0^-} = 0 \quad (23)$$

$$\beta_1 [T_1(0^+, t) - T^i] - \beta_2 [T_2(0^-, t) - T^i] \simeq 0 \quad (24)$$

We have cast the mathematical problem [Eqs. (19)–(24)] in non-dimensional form by selecting the solid-block half length



$a$ , the top-temperature transient time  $T$  and the initial temperature  $T^i$  as reference parameters for, respectively, coordinate  $y$ , time  $t$  and temperatures  $T_k$ . The characteristic numbers generated by this choice are tabulated in Table 1 together with the selected computational cases. We have set the diffusion numbers  $\rho_k c_k a^2 / \lambda_k T$  to unity for simplicity and have chosen the top-temperature increase as 10% of the initial temperature to be somehow consistent with the assumed validity of thermal-stress linearisation [Eq. (13)]. We have solved the mathematical non-dimensional problem

**Table 1** Computational cases and selected values of characteristic numbers

case	$\rho_k c_k a^2 / \lambda_k T$	$T^f / T^i$	$\lambda_2 / \lambda_1$	$\beta_2 / \beta_1$
1	1	1.1	1.0	1.0
2	1	1.1	0.5	1.0
3	1	1.1	0.5	0.9

numerically via two independently thought, time-accurate, finite-difference based algorithms (DG & PSL) independently implemented in fortran codes. The one-dimensional grid on the  $y/a$  axis comprises 102 points with a non-dimensional step of  $2 \cdot 10^{-2}$ ; the non-dimensional time step is  $5 \cdot 10^{-5}$ . The temperature-profile temporal evolutions to steady state for each computational case listed in Table 1 are shown in Figs. 8–10. The blue, red and green profiles corresponds to, respectively, the initial situation, the end of the top-temperature transient and the steady state. The time necessary to attain steady state is about twice the top-temperature transient duration. Case 1 (Fig. 8) reflects the standard situation with temperature and heat-flux continuity at the separation surface because the solids are made of same material; this case has been considered mainly to validate prediction capability of and agreement between the two independent numerical codes. Case 2 (Fig. 9) has been selected to reproduce the standard textbook result based on the intuitive imposition of temperature continuity [Eq. (2)]. The solids are made of different materials with different thermal behaviours ( $\lambda_2 / \lambda_1 = 0.5$ ) but differences in their stress response to thermal field are ignored by forcing  $\beta_2 / \beta_1 = 1$ ; consequently, temperature continuity with profile-slope discontinuity are recovered. This approximation is, therefore, meaningful only when the thermal-stress coefficients  $\beta_k$  are approximately equal. Case 3 (Fig. 10) corresponds to the more physical situation in which heat-flux [Eqs. (1) and (23)] and tension [Eqs. (11) and (24)] continuity prevail simultaneously at the separation surface; in this way, the materials' different stress responses to thermal field are taken into due account and, obviously, a temperature jump must settle in at the separation surface in accordance with Eq. (24) in order to secure tension continuity. The temperature jump at the separation

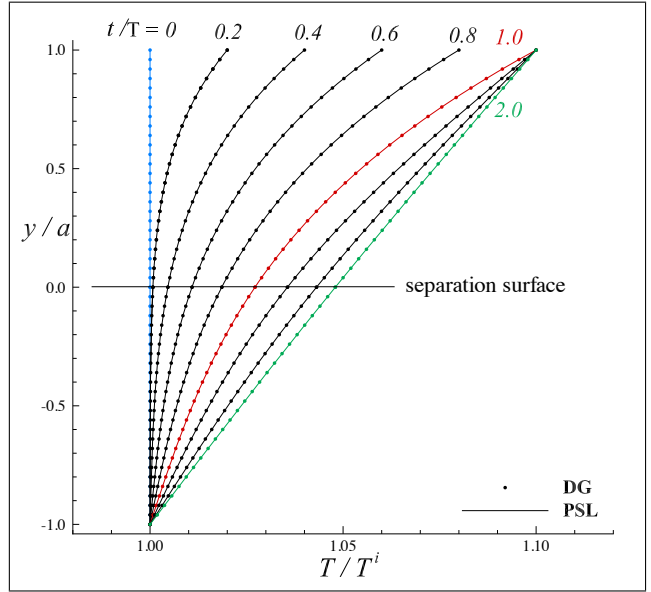


**Fig. 8** Computational case 1. Solids are made by same material.

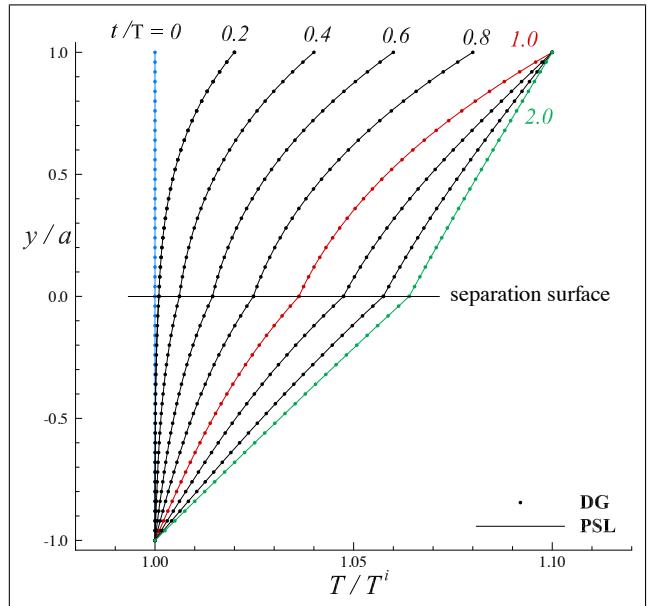


**Fig. 9** Computational case 2. Solids are made by different material but differences in thermal-stress behaviour are ignored; temperature continuity is imposed (forced) at separation surface.

surface shown in Fig. 10 may appear surprising to minds accustomed, by consuetude in years of practice, to the profile of Fig. 9; yet it is an effect guaranteed by the principle of momentum conservation as physically legitimate as the temperature-profile slope jump is guaranteed by the principle of energy conservation.

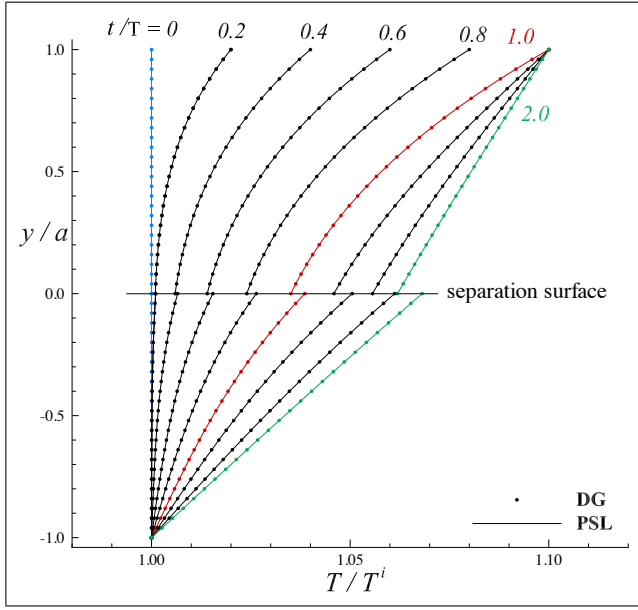


**Fig. 10** Computational case 3. Solids are made by different material and differences in thermal-stress behaviour are taken into account; temperature jump at separation surface is necessary to secure tension continuity.

## 4 Heat-transfer test case with interface

### 4.1 Theoretical considerations

In the presence of an interface (Figs. 4–5), the surface balance equations for mass, thermodynamic energy and momentum [93] for solids ( $\mathbf{v}_k = \tilde{\mathbf{v}} = \mathbf{w} = 0$ ) read

$$\frac{\partial \tilde{\rho}}{\partial t} = 0 \quad (25)$$

$$\tilde{\rho} \frac{\partial \tilde{u}}{\partial t} - \nabla_s \cdot [\mathbf{n} \times (\mathbf{n} \times \tilde{\mathbf{J}}_U)] = \mathbf{n}_1 \cdot \mathbf{J}_{U,1} + \mathbf{n}_2 \cdot \mathbf{J}_{U,2} \quad (26)$$

$$\nabla_s \cdot [\mathbf{n} \times (\mathbf{n} \times \tilde{\boldsymbol{\tau}})] = -\mathbf{n}_1 \cdot \boldsymbol{\tau}_1 - \mathbf{n}_2 \cdot \boldsymbol{\tau}_2 \quad (27)$$

In Eqs. (25)–(26)

- $\tilde{\rho}$  superficial mass density
- $\tilde{u}$  superficial thermodynamic-energy density
- $\tilde{\boldsymbol{\tau}}$  superficial stress tensor
- $\tilde{\mathbf{J}}_U$  superficial thermodynamic-energy diffusive flux

Equation (25) enforces the constancy of the superficial mass density, a consistent analog of what happens in the solids. Equations (26) and (27) stipulate unambiguously the lack of heat-flux and continuity tension. The heat-flux jump [right-hand side of Eq. (26)] provides the thermodynamic energy deposited per unit time in the interface's unit area which, in turn, is partly (algebraically) stored locally and partly

diffused *tangentially* along the interface. The tension jump [right-hand side of Eq. (27)] balances the superficial force arising from the tensional state existing inside the interface.

For consistency with the situation without interface, dealt with in Sec. 3, we retain same phenomenological relations [Eqs. (12) and (13)] for the solids. For the solid interface, we assume a Fourier-like superficial thermodynamic-energy diffusive flux [93]

$$\mathbf{n} \times (\mathbf{n} \times \tilde{\mathbf{J}}_U) = \tilde{\lambda}_s \nabla_s \tilde{T} \quad (28)$$

and a Hooke-like isotropic superficial stress tensor

$$\mathbf{n} \times (\mathbf{n} \times \tilde{\boldsymbol{\tau}}) \simeq \tilde{\beta}_s (\tilde{T} - \tilde{T}_0) \mathbf{U}_s \quad (29)$$

with neglected elastic contribution and linearised thermal stress for consistency with Eq. (13). In Eqs. (28) and (29)

- $\tilde{T}$  superficial temperature
- $\tilde{T}_0$  superficial reference temperature
- $\tilde{\lambda}_s$  superficial thermal conductivity (tangential)
- $\tilde{\beta}_s$  superficial thermal-stress coefficient (tangential)
- $\mathbf{U}_s$  surface unit tensor

Superficial thermal conductivity and thermal-stress coefficient are considered constant. Moreover, in line with the for-convenience assumed negligibility of deformations in both solids and solid interface, we retain for the superficial thermodynamic-energy density only the superficial-temperature dependence and assume constant the superficial constant-strain specific heat [28]

$$\tilde{u}(\tilde{T}) = \tilde{u}(\tilde{T}_0) + \tilde{c}(\tilde{T} - \tilde{T}_0) \quad (30)$$

On the basis of the described set of assumptions, the surface balance equations of thermodynamic energy and momentum [Eqs. (26) and (27)] acquire the closed form

$$\tilde{\rho} \tilde{c} \frac{\partial \tilde{T}}{\partial t} - \tilde{\lambda}_s \nabla_s^2 \tilde{T} = -\lambda_1 \mathbf{n}_1 \cdot \nabla T_1 - \lambda_2 \mathbf{n}_2 \cdot \nabla T_2 \quad (31)$$

$$\nabla_s \cdot [\tilde{\beta}_s (\tilde{T} - \tilde{T}_0) \mathbf{U}_s] \simeq \beta_1 (T_1 - T_{0,1})_{n=0^+} \mathbf{n}_1 + \beta_2 (T_2 - T_{0,2})_{n=0^-} \mathbf{n}_2 \quad (32)$$

The terms on the right-hand side of Eqs. (31) and (32) are intended evaluated at the generic point  $P$  of the interface (see Figs. 4 and 5).

### 4.2 Planar configuration

#### 4.2.1 Differential equations and initial/boundary conditions

With reference to Fig. 4, we complement the still applicable initial and boundary conditions [Eqs. (18)–(21)] and the heat-transfer equations [Eq. (22)] considered in Sec. 3.2 with the following:

– adiabatic vertical walls

$$\left(\frac{\partial \tilde{T}}{\partial x}\right)_{x=\pm a} = \left(\frac{\partial \tilde{T}}{\partial z}\right)_{z=\pm a} = 0 \quad (33)$$

– uniform initial temperature

$$\tilde{T}(x, z, 0) = T^i \quad (34)$$

The surface balance equations [Eqs. (31) and (32)] become

$$\tilde{\rho} \tilde{c} \frac{\partial \tilde{T}}{\partial t} - \tilde{\lambda}_s \nabla_s^2 \tilde{T} = \lambda_1 \left(\frac{\partial T_1}{\partial y}\right)_{y=0^+} - \lambda_2 \left(\frac{\partial T_2}{\partial y}\right)_{y=0^-} \quad (35)$$

$$\tilde{\beta}_s \nabla_s \tilde{T} \simeq -\beta_1 [T_1(0^+, t) - T^i] \mathbf{j} + \beta_2 [T_2(0^-, t) - T^i] \mathbf{j} \quad (36)$$

The projection of Eq. (36) in the  $x$  and  $z$  directions yields

$$\frac{\partial \tilde{T}}{\partial x} = \frac{\partial \tilde{T}}{\partial z} \simeq 0 \quad (37)$$

Thus, within the current approximation, the superficial temperature must be uniform along the interface, its surface gradient vanishes and so does its surface Laplacian operator

$$\nabla_s^2 \tilde{T} = \nabla_s \cdot \nabla_s \tilde{T} = \frac{\partial^2 \tilde{T}}{\partial x^2} + \frac{\partial^2 \tilde{T}}{\partial z^2} \simeq 0 \quad (38)$$

In this case, therefore, the tangential diffusion of superficial thermodynamic energy is switched off. With these simplifications, Eqs. (35) and (36) can be reduced to the final form

$$\tilde{\rho} \tilde{c} \frac{\partial \tilde{T}}{\partial t} = \lambda_1 \left(\frac{\partial T_1}{\partial y}\right)_{y=0^+} - \lambda_2 \left(\frac{\partial T_2}{\partial y}\right)_{y=0^-} \quad (39)$$

$$\beta_1 [T_1(0^+, t) - T^i] - \beta_2 [T_2(0^-, t) - T^i] \simeq 0 \quad (40)$$

Equation (40) is the same as Eq. (24) and indicates that thermal-stress continuity prevails also in the presence of a planar interface because the tensional state in the interface does not generate any stress in the normal direction; this is a consequence of the absence of interface curvature, as it will appear clear in Sec. 4.3.1.

The comparison of Eqs. (39) and (40) with Eqs. (23) and (24) clearly reveals that the mathematical problem we have built so far in the presence of the interface is underdetermined: one equation is missing because the number (two) of interface conditions is the same as in the case of a separation surface but Eq. (39) contains the time derivative of the superficial temperature, a variable that belongs to the set of unknowns of the mathematical problem. The occurrence of such a situation is not new. A quick check in the literature reveals that differential/algebraic equations are somehow assumed or derived in addition to the surface balance

equations. In the case of fluid interfaces, for example, Waldmann [136] selected

$$\frac{1}{\tilde{T}} = \frac{1}{2} \left( \frac{1}{T_1} + \frac{1}{T_2} \right) \quad (41)$$

Bedeaux and co-authors [14] used arguments of LIT to derive an additional differential equation [Eq. (5.14) at page 454] for the superficial temperature that reduces to the algebraic form

$$\tilde{T} = \frac{1}{2} (T_1 + T_2) \quad (42)$$

in a zero-order approximation. These authors derive an interesting surface entropy-production expression [Eq. (4.16) at page 451] that contains the normal heat fluxes of the volume phases. Obviously, phenomenological equations for the latter terms are provided by the LIT analysis of the entropy productions in the *volume* phases; instead, and rather peculiarly, the authors seemingly ignore this fact and proceed to derive from the *surface* entropy production, always according to the LIT prescript, additional phenomenological equations for the terms in question, their belonging to the volume phases notwithstanding. A similar approach appears to have been followed also by Sagis [113] within the formalism of extended irreversible thermodynamics. If Bedeaux and co-authors would have looked at their surface-entropy production from the viewpoint that Napolitano [93] exploited to prove the coincidence of the normal components of, respectively, the superficial mass velocity and the interface geometrical velocity ( $\mathbf{n} \cdot \tilde{\mathbf{v}} = \mathbf{n} \cdot \mathbf{w}$ ) then they would have retrieved for the interface they considered the condition of temperature continuity  $\tilde{T} = T_1 = T_2$ . Napolitano himself dealt with *pure* interfaces [92] under the assumption that (Sec. 2 at page 567)

the interface ... is considered a stream surface across which the velocity and the temperature are continuous.

that is equivalent to complement the surface balance equations with additional algebraic equations. This important aspect of MTGSI is still an open issue dealt with in different manners and a final word converting workers in the field to unanimous consensus seems to have not been spoken yet. We are aware that the resolution of the hindrance caused by such an aspect is crucial, essential and mandatory for a satisfactory establishment of MTGSI but here we will not deal with it because it is not critical for the modest purposes of this work. In Sec. 4.2.2 we will derive the missing equation following a conceptual pathway whose end products are consistent (to our minds) with the surface balance equations dealt with so far [Eqs. (39) and (40)]; then, we will proceed in Sec. 4.2.3 to present and discuss numerical results.

#### 4.2.2 Derivation of the missing equation

We begin from the configuration illustrated in Fig. 11: three solids ( $k = 1, \sim, 2$ ) in contact with separation surfaces as considered in Sec. 3. For the solid in the middle ( $k = \sim$ ), we extend a bit the phenomenological equations [Eqs. (12) and (13)] assumed for the other solids ( $k = 1, 2$ ): the thermal-conductivity tensor and the thermal-stress-coefficient tensor are still diagonal but not isotropic

$$\mathbf{J}_{V, \sim} = -(\lambda_{\sim s} \mathbf{U}_s + \lambda_{\sim n} \mathbf{n}_{\sim} \mathbf{n}_{\sim}) \cdot \nabla T_{\sim} \quad (43)$$

$$\boldsymbol{\tau}_{\sim} \simeq -(\beta_{\sim s} \mathbf{U}_s + \beta_{\sim n} \mathbf{n}_{\sim} \mathbf{n}_{\sim})(T_{\sim} - T^i) \quad (44)$$

The symbol  $\sim$  appears as subscript for the time being in analogy with the other two volume phases. This position is meant to single out diffusion processes in the normal direction with respect to those in the tangential directions and seems legitimate in view of the forthcoming passage to the limit  $\epsilon \rightarrow 0$ . Heat-flux continuity

$$\lambda_1 \mathbf{n}_1 \cdot \nabla T_1|_{+\epsilon, t} + \lambda_{\sim n} \mathbf{n}_{\sim} \cdot \nabla T_{\sim}|_{+\epsilon, t} = 0 \quad (45)$$

$$\lambda_2 \mathbf{n}_2 \cdot \nabla T_2|_{-\epsilon, t} - \lambda_{\sim n} \mathbf{n}_{\sim} \cdot \nabla T_{\sim}|_{-\epsilon, t} = 0 \quad (46)$$

and tension continuity

$$\beta_1 [T_1(+\epsilon, t) - T^i] \mathbf{n}_1 \cdot \mathbf{U} + \beta_{\sim n} [T_{\sim}(+\epsilon, t) - T^i] \mathbf{n}_{\sim} \cdot \mathbf{U} = 0 \quad (47)$$

$$\beta_2 [T_2(-\epsilon, t) - T^i] \mathbf{n}_2 \cdot \mathbf{U} - \beta_{\sim n} [T_{\sim}(-\epsilon, t) - T^i] \mathbf{n}_{\sim} \cdot \mathbf{U} = 0 \quad (48)$$

apply at the points of the upper/lower separation surfaces. In planar configuration, Eqs. (45)–(48) can be rephrased more explicitly as

$$\lambda_1 \left( \frac{\partial T_1}{\partial y} \right)_{y=+\epsilon} = \lambda_{\sim n} \left( \frac{\partial T_{\sim}}{\partial y} \right)_{y=+\epsilon} \quad (49)$$

$$\lambda_2 \left( \frac{\partial T_2}{\partial y} \right)_{y=-\epsilon} = \lambda_{\sim n} \left( \frac{\partial T_{\sim}}{\partial y} \right)_{y=-\epsilon} \quad (50)$$

and

$$\beta_1 [T_1(+\epsilon, t) - T^i] - \beta_{\sim n} [T_{\sim}(+\epsilon, t) - T^i] = 0 \quad (51)$$

$$\beta_2 [T_2(-\epsilon, t) - T^i] - \beta_{\sim n} [T_{\sim}(-\epsilon, t) - T^i] = 0 \quad (52)$$

The heat transfer through the solid  $\sim$  is governed by the differential equation

$$\rho_{\sim} c_{\sim} \frac{\partial T_{\sim}}{\partial t} = \lambda_{\sim n} \frac{\partial^2 T_{\sim}}{\partial y^2} \quad (53)$$

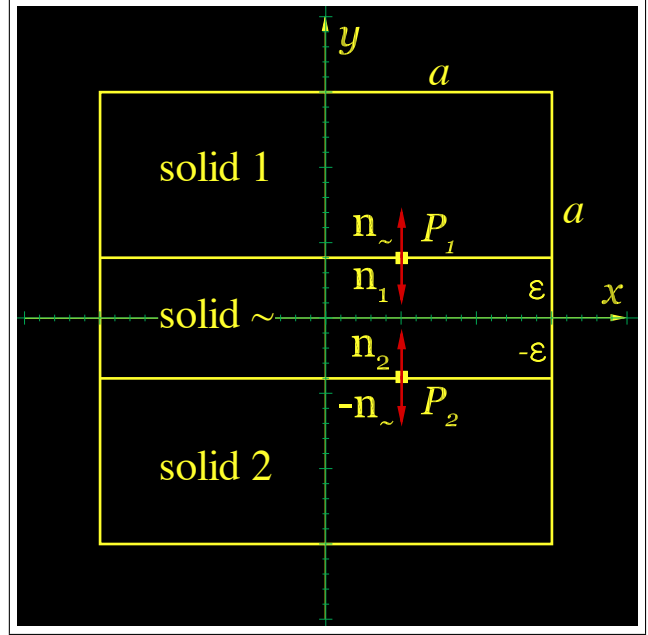


**Fig. 11** Alternative macroscopic representation of the silicon-platinum contact sketched in Fig. 3 when  $\epsilon \rightarrow 0$

The integration of Eq. (53) along  $y$  from  $-\epsilon$  to  $+\epsilon$  yields

$$\rho_{\sim} c_{\sim} \int_{-\epsilon}^{+\epsilon} \frac{\partial T_{\sim}}{\partial t} dy = \lambda_{\sim n} \int_{-\epsilon}^{+\epsilon} \frac{\partial^2 T_{\sim}}{\partial y^2} dy \quad (54)$$

The time derivative commutes with the integral and the term on the right-hand side is easily integrated

$$\rho_{\sim} c_{\sim} \frac{\partial}{\partial t} \int_{-\epsilon}^{+\epsilon} T_{\sim} dy = \lambda_{\sim n} \left( \frac{\partial T_{\sim}}{\partial y} \right)_{y=+\epsilon} - \lambda_{\sim n} \left( \frac{\partial T_{\sim}}{\partial y} \right)_{y=-\epsilon} \quad (55)$$

We introduce the average temperature

$$\langle T_{\sim} \rangle_{\epsilon} = \frac{1}{2\epsilon} \int_{-\epsilon}^{+\epsilon} T_{\sim} dy \quad (56)$$

and take advantage now of heat-flux continuity [Eqs. (49) and (50)] on both separation surfaces to recast Eq. (55) into the equivalent form

$$(2\epsilon \rho_{\sim}) c_{\sim} \frac{\partial \langle T_{\sim} \rangle_{\epsilon}}{\partial t} = \lambda_1 \left( \frac{\partial T_1}{\partial y} \right)_{y=+\epsilon} - \lambda_2 \left( \frac{\partial T_2}{\partial y} \right)_{y=-\epsilon} \quad (57)$$

which, passed to the limit  $\epsilon \rightarrow 0$ , assumes the structure of Eq. (39) and, by comparison, leads to the following definitions

$$\lim_{\epsilon \rightarrow 0} (2\epsilon \rho_{\sim}) = \tilde{\rho} \quad (58)$$

$$\lim_{\epsilon \rightarrow 0} c_{\sim} = \tilde{c} \quad (59)$$

$$\lim_{\epsilon \rightarrow 0} \langle T_{\sim} \rangle_{\epsilon} = \tilde{T} \quad (60)$$

The existence of the limits defined by Eqs. (58)–(60) may seem a strong assumption but, on the other hand, its justification is prompted by the fact that it sanctions the mathematical equivalence between Eqs. (39) and (57). Next, we turn to the tension-continuity boundary conditions [Eqs. (51) and (52)]: mathematically speaking, they are two independent equations and we can recast them by subtraction/addition into the equivalent, and obviously still independent, forms

$$\beta_{\sim n} [T_{\sim}(+\epsilon, t) - T^i] - \beta_{\sim n} [T_{\sim}(-\epsilon, t) - T^i] = \beta_1 [T_1(+\epsilon, t) - T^i] - \beta_2 [T_2(-\epsilon, t) - T^i] \quad (61)$$

$$\beta_{\sim n} [T_{\sim}(+\epsilon, t) - T^i] + \beta_{\sim n} [T_{\sim}(-\epsilon, t) - T^i] = \beta_1 [T_1(+\epsilon, t) - T^i] + \beta_2 [T_2(-\epsilon, t) - T^i] \quad (62)$$

If we pass Eq. (61) to the limit  $\epsilon \rightarrow 0$  then we re-obtain Eq. (40). Equation (62) is still exploitable and its adequate manipulation leads to the missing equation we are looking for to close our mathematical problem. We accomplish this task by rewriting the left-hand side of Eq. (62) as

$$\beta_{\sim n} [T_{\sim}(+\epsilon, t) - \langle T_{\sim} \rangle_{\epsilon}] + \beta_{\sim n} [T_{\sim}(-\epsilon, t) - \langle T_{\sim} \rangle_{\epsilon}] + 2\beta_{\sim n} [\langle T_{\sim} \rangle_{\epsilon} - T^i] = \beta_1 [T_1(+\epsilon, t) - T^i] + \beta_2 [T_2(-\epsilon, t) - T^i] \quad (63)$$

and then passing to the limit  $\epsilon \rightarrow 0$ . In so doing, we assume reasonably that

$$\lim_{\epsilon \rightarrow 0} [T_{\sim}(\pm\epsilon, t) - \langle T_{\sim} \rangle_{\epsilon}] = 0 \quad (64)$$

we register the definition

$$\lim_{\epsilon \rightarrow 0} \beta_{\sim n} = \tilde{\beta}_n \quad (65)$$

and consequently obtain the missing equation

$$2\tilde{\beta}_n (\tilde{T} - T^i) = \beta_1 [T_1(0^+, t) - T^i] + \beta_2 [T_2(0^-, t) - T^i] \quad (66)$$

that must be associated to Eqs. (39) and (40). It ought to be noticed that Eq. (66) reduces to the result [Eq. (42)] of Bédard and co-authors [14] in the particular case  $\tilde{\beta}_n = \beta_1 = \beta_2$ . An incidental remark is due at this point. After having seen how useful addition between Eqs. (51) and (52) is for the purpose of obtaining the missing equation, the attentive reader may have noticed that, as a matter of fact, we took advantage of the subtraction between Eqs. (49) and (50) to obtain Eq. (57) and be wondering what happens instead in

case of addition. It is a legitimate observation with a straightforward answer. Skipping the algebra, the mentioned operation together and the subsequent passage to the limit  $\epsilon \rightarrow 0$  generates the following equation

$$\lim_{\epsilon \rightarrow 0} \left[ \lambda_{\sim n} \left( \frac{\partial T_{\sim}}{\partial y} \right)_{y=+\epsilon} + \lambda_{\sim n} \left( \frac{\partial T_{\sim}}{\partial y} \right)_{y=-\epsilon} \right] = \lambda_1 \left( \frac{\partial T_1}{\partial y} \right)_{y=0^+} + \lambda_2 \left( \frac{\partial T_2}{\partial y} \right)_{y=0^-} \quad (67)$$

Equation (67) is certainly another equations but is unhelpful because it introduces also an additional unknown, that is, the quantity on its left-hand side, which does not intervene in any other place in the set of governing equations. This *additional* equation is, therefore, a mathematical blind alley and is not needed.

Coming back to Eq. (66), we looked at it, stepped back for a thoughtful moment and wondered about its physical meaning. More importantly, we asked ourselves if there is a more physically profound way to deduce it rather than our *ad-hoc* manner. This is, of course, a very interesting and captivating problem but we felt it is a bit outside the reach of our preliminary study; therefore, for the time being, we decided to stamp the problem as *future work* (Sec. 5) and to carry on with the numerical calculations.

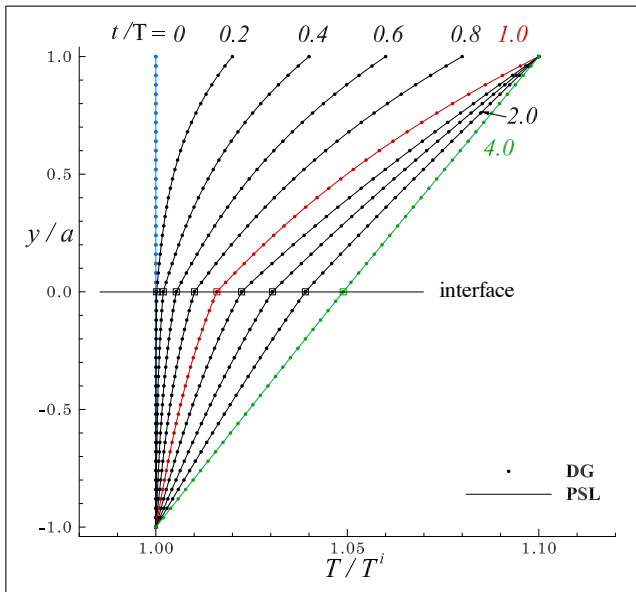
#### 4.2.3 Results

With the aid of Eq. (66), our mathematical problem is thus closed and we have cast it in non-dimensional form with the same reference parameters selected in Sec. 3.2 [see text after Eq. (24)]. Two other characteristic numbers appear in addition to those tabulated in Table 1; they contain physical variables related to the interface and are shown in the rightmost columns of Table 2 which lists also the selected computational cases. The temperature-profile temporal evolutions corresponding to these computational cases are illustrated in Figs. 12–17. We recall the colour convention: blue, red and green profiles corresponds to, respectively, initial situation, end of the top-temperature transient and steady state, respectively. The time necessary to attain steady state is about four times the top-temperature transient duration, therefore twice as long the time required to achieve steady state without interface. The square symbols indicate the values of  $\tilde{T}/T^i$  (results from both numerical codes superpose very precisely). Cases 1-3 are analogous to the those analysed in Sec. 3.2 (see Table 1) and have been considered to put in evidence the effects due to the presence of the interface. In case 1 (Fig. 12), the temperature-profile slopes at the interface show a clear difference, notwithstanding that  $\lambda_2/\lambda_1 = 1$ , in accordance with Eq. (39): the heat-flux difference (right-hand side) feeds into the superficial thermodynamic energy (left-hand side) and slope continuity is re-

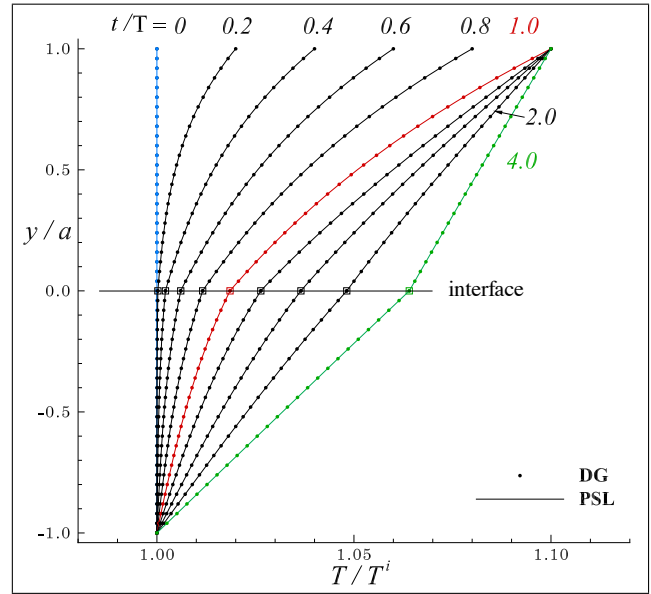
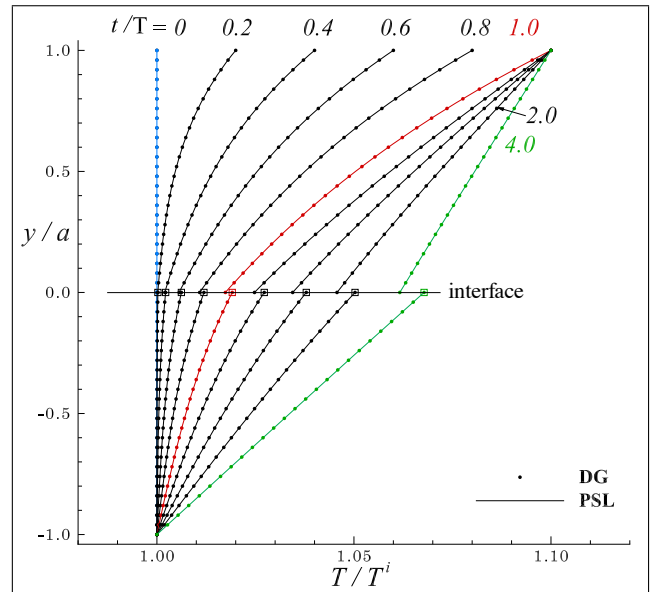
**Table 2** Computational cases and selected values of characteristic numbers

case	$\rho_k c_k a^2 / \lambda_k T$	$T^f / T^i$	$\lambda_2 / \lambda_1$	$\beta_2 / \beta_1$	$\tilde{\rho} \tilde{c} a / \lambda_1 T$	$\tilde{\beta}_n / \beta_1$
1	1	1.1	1.0	1.0	1	1.0
2	1	1.1	0.5	1.0	1	1.0
3	1	1.1	0.5	0.9	1	0.9
4	1	1.1	0.5	0.9	1	1.0
5	1	1.1	0.5	1.1	1	0.9
6	1	1.1	1.0	1.0	1	$\ll 1$

covered only with the steady-state attainment. The continuity of *all* temperatures at the interface is a consequence of the assumption that the interface stress response to thermal field is similar to the one ( $\beta_2 / \beta_1 = \tilde{\beta}_n / \beta_1 = 1$ ) of the material composing the solids 1 and 2. It constitutes a further evidence of validation for our numerical codes because it can be verified analytically from Eqs. (40) and (66). The temperature-profile evolutions for case 2 (Fig. 13), case

**Fig. 12** Computational case 1. Solids are made by same material.

3 (Fig. 14) and case 4 (Fig. 15) show consistent behaviour. The interface temperature in cases 3 and 4 coincides with, respectively,  $T_2(0^+, t)$  and  $T_1(0^+, t)$  because  $\tilde{\beta}_n = \beta_2$  in the former case and  $\tilde{\beta}_n = \beta_1$  in the latter case. Case 5 (Fig. 16) is really interesting from a physical point of view and, at the same time, significant from an engineering point of view. The temperature profiles in Figs. 14 and 16, when compared with the temperature profiles of Fig. 10, provide clear evidence of the thermal protection action of the interface on solid 2. In order to emphasise such evidence, we have collected in Table 3 meaningful values of temperatures and heat

**Fig. 13** Computational case 2. Solids are made by different material but differences in thermal-stress behaviour are ignored; temperature continuity is imposed (forced) at interface. Superficial-temperature coincidence with solids' temperatures is a consequence.**Fig. 14** Computational case 3. Solids are made by different material and differences in thermal-stress behaviour are taken into account; temperature jump at interface is necessary to secure tension continuity. Superficial temperature coincides with that of solid 2 because  $\tilde{\beta}_n = \beta_2$ .

fluxes at steady state ( $t/T \simeq 2$  for case 3<sup>a</sup> and  $t/T \simeq 4$  for cases 3<sup>b</sup> and 5) for comparison. The presence of the interface mitigates the heat flux received by solid 2 (rightmost column in Table 3) as much as 15 % between cases 3<sup>a</sup> and 5. Case 6 (Fig. 17) represents the extreme, and therefore ideal, situation when  $\tilde{\beta}_n \ll \beta_1 = \beta_2$ . In this case, the thermal-protection action of the interface is complete: solid 2 is totally shielded and does not receive any heat flux because the



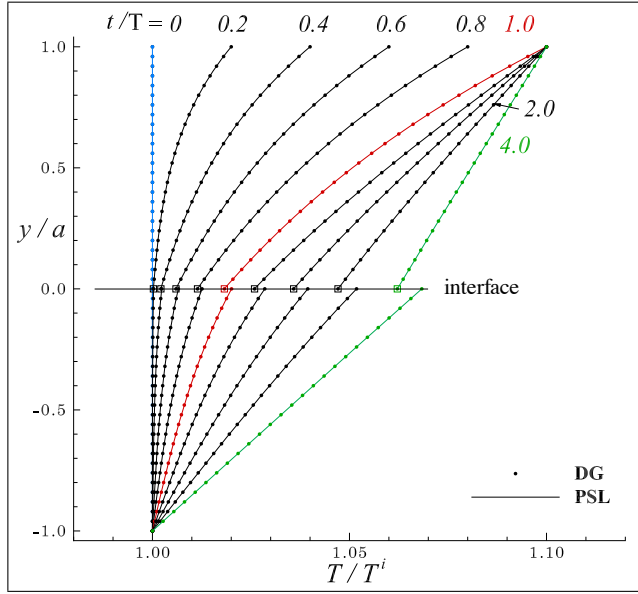


**Fig. 15** Computational case 4. Similar to case 3 but superficial temperature coincides with that of solid 1 because  $\tilde{\beta}_n = \beta_1$ .

**Table 3** Comparison of selected values of temperatures and heat fluxes at steady state

case	$T_1(0^+)/T^i$	$\frac{a}{T^i} \left( \frac{\partial T_1}{\partial y} \right)_{0^+}$	$\tilde{T}/T^i$	$T_2(0^-)/T^i$	$\frac{a}{T^i} \left( \frac{\partial T_2}{\partial y} \right)_{0^-}$
3 <sup>a</sup>	1.062	$3.548 \cdot 10^{-2}$		1.068	$7.097 \cdot 10^{-2}$
3 <sup>b</sup>	1.062	$3.740 \cdot 10^{-2}$	1.068	1.068	$6.886 \cdot 10^{-2}$
5	1.065	$3.368 \cdot 10^{-2}$	1.072	1.059	$6.029 \cdot 10^{-2}$

<sup>a</sup> without interface (Table 1)

<sup>b</sup> with interface (Table 2)

heat flux outgoing from solid 1 goes exclusively to replenish the superficial thermodynamic energy of the interface whose superficial temperature grows monotonically with time even after the attainment of the steady state ( $t/T \simeq 1.5$ ) in solid 1 (solid squares). The results shown in Fig. 17 are analogous to and confirm those obtained by Schmidtman [116] with a physically simpler model.

### 4.3 Cylindrical configuration

#### 4.3.1 Differential equations and initial/boundary conditions

For the cylindrical configuration (see Fig. 5), we adopt body-fitted coordinates: the curvilinear abscissa  $s$  reckoned from point A and the normal distance  $n$  from the interface (positive/negative in solid 1/2). We assume

- uniform initial temperature

$$T_k(s, n, z, 0) = \tilde{T}(s, z, 0) = T^i \quad (68)$$

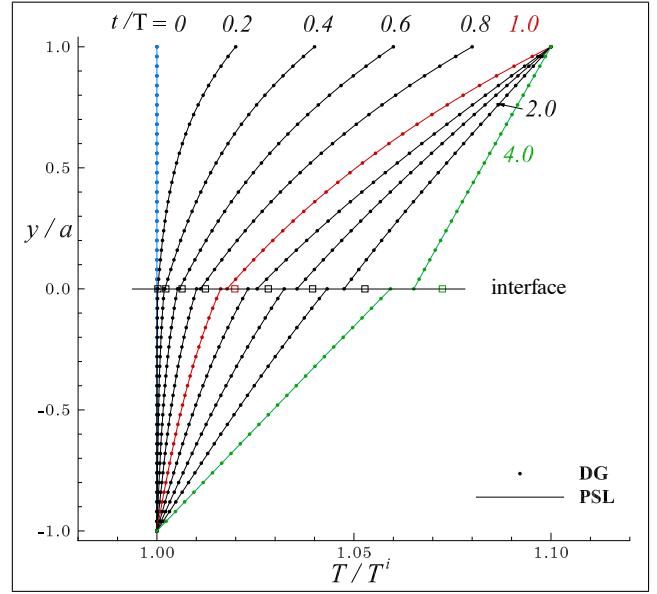


**Fig. 16** Computational case 5. Solids are made by different material and differences in thermal-stress behaviour are taken into account; temperature jump at separation surface is necessary to secure tension continuity. Superficial temperature governed by heat-flux difference at interface according to Eq. (39).

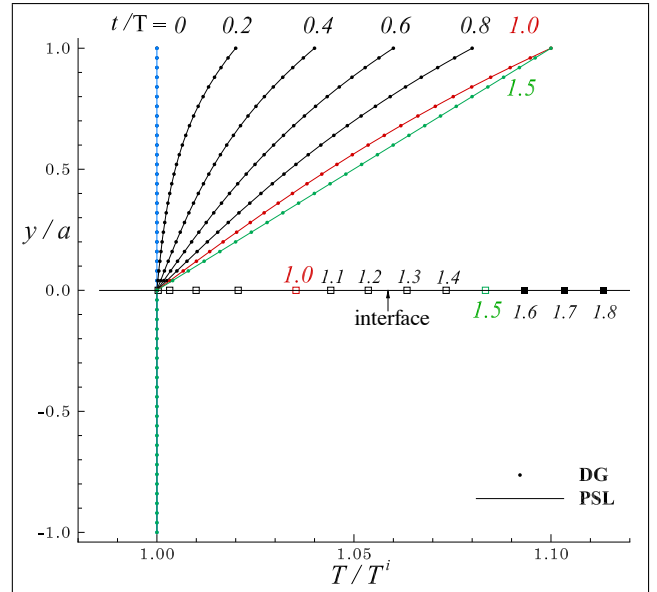


**Fig. 17** Computational case 6. Ideal situation of complete thermal protection when  $\tilde{\beta}_n \ll \beta_1 = \beta_2$ , analogous to the case studied by Schmidtman [116].

- uniform temperature at the top of solid 1 increasing linearly in time, within a finite interval  $T$ , from the initial value  $T^i$  to a final value  $T^f$

$$T_1(s, +R, z, t) = \begin{cases} T^i & t < 0 \\ T^i + (T^f - T^i) \frac{t}{T} & 0 \leq t \leq T \\ T^f & T < t \end{cases}$$

(69)

These conditions determine an one-dimensional heat transfer in the radial direction governed by the standard diffusion equation

$$\rho_k c_k \frac{\partial T_k}{\partial t} = \lambda_k \frac{\partial^2 T_k}{\partial n^2} + \frac{\lambda_k}{n+R} \frac{\partial T_k}{\partial n} \quad (70)$$

Equation (70) must be handled with care on the cylinder axis ( $n = -R$ ;  $k = 2$ ) because the scale factor in the denominator of the second term on the right-hand side vanishes. In order to avoid the discontinuity, therefore, we must assume the ulterior boundary condition

$$\left( \frac{\partial T_2}{\partial n} \right)_{n=-R} = 0 \quad (71)$$

Consequently, the second term on the right-hand side becomes a mathematically undetermined form resolvable by the de l'Hôpital's theorem

$$\lim_{n \rightarrow -R} \frac{1}{n+R} \frac{\partial T_2}{\partial n} = \left( \frac{\partial^2 T_2}{\partial n^2} \right)_{n=-R} \quad (72)$$

and the governing equation [Eq. (70)] becomes discontinuity-free

$$\rho_2 c_2 \left( \frac{\partial T_2}{\partial t} \right)_{n=-R} = 2\lambda_2 \left( \frac{\partial^2 T_2}{\partial n^2} \right)_{n=-R} \quad (73)$$

The surface balance equations [Eqs. (31) and (32)] become

$$\tilde{\rho} \tilde{c} \frac{\partial \tilde{T}}{\partial t} - \tilde{\lambda}_s \nabla_s^2 \tilde{T} = \lambda_1 \left( \frac{\partial T_1}{\partial n} \right)_{n=0^+} - \lambda_2 \left( \frac{\partial T_2}{\partial n} \right)_{n=0^-} \quad (74)$$

$$\tilde{\beta}_s \nabla_s \tilde{T} - \frac{\tilde{\beta}_s}{R} (\tilde{T} - T^i) \mathbf{e}_n \simeq -\beta_1 [T_1(0^+, t) - T^i] \mathbf{e}_n + \beta_2 [T_2(0^-, t) - T^i] \mathbf{e}_n \quad (75)$$

From the comparison between Eqs. (36) and (75), we notice the appearance of the interface-curvature effect on the left-hand side of Eq. (75): the tensional state *inside* the curved interface features a tension component *outside* of the interface itself in the normal direction, an interesting although peculiar physical occurrence already encountered by Laplace during his studies on capillarity [79] slightly more than 200 years ago, that removes the continuity of volume-phase tensions [recall text in Sec. 4.2.1 after Eq. (40)]. Once again, the projection of Eq. (75) along tangential and axial directions informs that the superficial temperature must be uniform along the interface

$$\frac{\partial \tilde{T}}{\partial s} = \frac{\partial \tilde{T}}{\partial z} \simeq 0 \quad (76)$$

so that its surface gradient and Laplacian operator vanish

$$\nabla_s^2 \tilde{T} = \nabla_s \cdot \nabla_s \tilde{T} = \frac{\partial^2 \tilde{T}}{\partial s^2} + \frac{\partial^2 \tilde{T}}{\partial z^2} \simeq 0 \quad (77)$$

Even for curved interface, therefore, the tangential diffusion of superficial thermodynamic energy is switched off. With these simplifications, Eqs. (74) and (75) can be reduced to the final form

$$\tilde{\rho} \tilde{c} \frac{\partial \tilde{T}}{\partial t} = \lambda_1 \left( \frac{\partial T_1}{\partial n} \right)_{n=0^+} - \lambda_2 \left( \frac{\partial T_2}{\partial n} \right)_{n=0^-} \quad (78)$$

$$\frac{\tilde{\beta}_s}{R} (\tilde{T} - T^i) \simeq \beta_1 [T_1(0^+, t) - T^i] - \beta_2 [T_2(0^-, t) - T^i] \quad (79)$$

Of course, we face now the same situation encountered with the planar interface: we need one additional equation. For this purpose, we have exported the reasoning based on the configuration illustrated in Fig. 11 to the cylindrical configuration shown in Fig. 5 and have retrieved again Eq. (66); we omit here the detailed algebra because its development follows smoothly guidelines similar to those described in Sec. 4.2.2 for the planar interface.

The mathematical problem cast in non-dimensional form features the same characteristic numbers shown in Table 2 but with a simple variation: the characteristic length  $a$  belonging to the planar interface must be replaced with the internal-solid radius  $R$ . The curvature term on the left-hand side of Eq. (75) generates the additional characteristic number  $\tilde{\beta}_s/\beta_1 R$ .

#### 4.3.2 Results

The major purpose to investigate the cylindrical configuration shown in Fig. 5 consists in emphasising the impact of the interface curvature on the thermal fields. Accordingly, we have selected as baseline the computational case 1 in Table 2, relative to planar interface, whose results are shown in Fig. 12: the solids are made by same material, their and the interface's stress response to thermal field is similar ( $\beta_1 = \beta_2 = \tilde{\beta}_n$ ), the flatness of the interface presupposes tension continuity [Eq. (40)] which, in combination with the additional equation [Eq. (66)], implies all-temperature continuity [ $\tilde{T}(t) = T_1(0^+, t) = T_2(0^-, t)$ ]. At steady state, the temperature profile is a straight line and the interface is basically *transparent*. We have repeated the calculation for the cylindrical configuration with the same values of the characteristic numbers of case 1 in Table 2 and with  $\tilde{\beta}_s/\beta_1 R = 0.1$  and have found out that the situation is different for a curved interface because the presence of the curvature breaks down tension continuity [Eq. (75)] with the remarkable outcome that temperature continuity does not settle in even for solids made by same material. This occurrence is clearly indicated by the temperature profiles shown in Fig. 18. At steady state, the heat flux vanishes everywhere and the temperature profiles are uniform. The external solid reaches the final temperature ( $T/T^i = 1.1$ ) imposed on its external circumference ( $n/R = 1$ ) but the internal solid remains a bit cooler

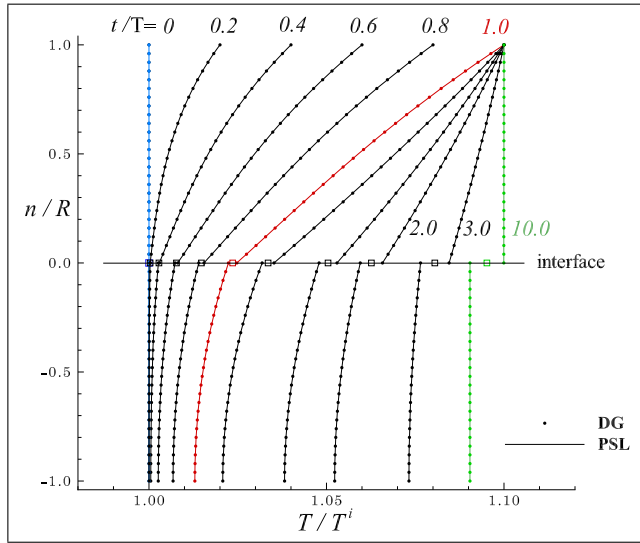


**Fig. 18** Computational case 1 of Table 2 for the cylindrical configuration of Fig. 5. Curvature characteristic number  $\tilde{\beta}_s/\beta_1 R = 0.1$ .

( $T/T^i \simeq 1.09$ ) because a fraction of the thermodynamic energy transported by diffusion during the transient is absorbed by the interface. The absorption process [Eq. (78)] is reflected in the interface-temperature (squares in Fig. 18) growth, in this case as the mean value between the temperatures of the solids, with final settling at a steady-state value  $\tilde{T}/T^i \simeq 1.095$ . The thermal protection exercised by the interface on the internal solid is evident and consistent with the one illustrated in Fig. 16 for the planar interface and for different materials.

## 5 Conclusions

The tentative application of the phenomenological theory of interfacial interactions to our *demonstrator* heat-transfer test case has shed constructive light on several aspects.

In the absence of interfaces (Sec. 3), it has brought forth, and helped us to understand, the importance of tension continuity [Eq. (11)] as physical boundary condition on the same footing of heat-flux continuity [Eq. (1)]. In our test case, Eq. (11) governs unequivocally the establishment of the temperature jump at the separation surface between the solids (Fig. 10). With our minds prejudiced by the standardly enforced temperature-continuity boundary condition [Eq. (2)], we received this result with a bit of justified hesitation and decided, therefore, to seek alternative and independent confirmation via MD calculations. These were performed by our collaborators in the technical university of Eindhoven and the details will be published soon in a dedicated article [96]; here we only anticipate that the MD results are in very good agreement with those produced by our calculations and, above all, confirm the temperature jump at the

separation surface. The MD intervention proved decisive to remove doubts and hesitation and we certainly look forward to its, hopefully forthcoming, fundamental support to obtain the necessary thermophysical properties of the interfaces. We are (now) convinced about the key role owned by the tension-continuity boundary condition and the physical significance of results generated by its imposition; we also believe and foresee that it will produce novel, unexpected, and far reaching consequences when enforced in fluid-dynamics contexts with fluids in contact with solids.

In the presence of interfaces (Sec. 4), the phenomenological-theory idea flourishes into a self-contained theoretical elaboration that, in our opinion, goes a long way in the direction of the “closed theories which could a priori predict ... catalytic properties” predicated by Kovalev and Kolesnikov [74]. All parameters called for in the elaboration have physical foundation and, remarkably, there is no place and no need for any heuristic empirical construct such as the ACs. Of course, we have enforced simplifying assumptions about those parameters but exclusively for the sake of simplicity in numerical calculations, a reasonable justification, and certainly never imperiling, to the best of our understanding, their physical meaningfulness. We believe that the quantitative results described and discussed in Secs. 4.2.3 and 4.3.2 are encouraging; they provide ulterior evidence of the phenomenological-theory predictive power and of how its physical parameters control the interface role as provider of thermal either protection or amplification. Therefore, we feel comfortable to conclude that they support convincingly our MTGSI research program and make worthwhile further investigation along its conceptual pathway. It is true that, for the time being, our theoretical elaboration shares the important problem related to the correct closure of the surface balance equations, introduced in Sec. 4.2.1, with predecessors in other application domains but, given the preliminary nature of our study, we have considered acceptable for our test case to overcome the problem as described in Sec. 4.2.2 without going (yet) into deeper details. Indeed, we have not investigated the possible ramifications and implications of the surface-entropy balance equation which has already proven useful *to fix* conceptual uncertainties [14,56,93,113]. We are obviously conscious of the importance of such a problem, are confident in the invaluable help harvestable from in-depth familiarisation with the pertinent literature and are prepared to confront it head-on in our future work of more fluid-dynamics nature that will concentrate on the MTGSI-idea application to a two-dimensional flow past a cylinder with and without interface, as sketched in Fig. 7.

**Acknowledgements** One of the authors (DG) wishes to dedicate his contribution in this work to his former student Birte Schmidtman [116] whose efforts should have been better recognised instead of be-

ing received with undeserved unscientific mistreatment when she presented physically consistent and correct results, although limited by simple modeling, that have been confirmed in full by the more complete physical model described in this work. The contributions of P. Solano-López and J. M. Donoso have been supported by the ESA TRP contract no. 4000112582/14/NL/PA titled “Novel methodology for gas-surface interactions in hypersonic reentry flows”.

## References

- Aifantis, E.C.: On the problem of diffusion in solids. *Acta Mechanica* **37**, 265–296 (1980)
- Ala-Nissila, T., Ferrando, R., Ying, S.C.: Collective and single particle diffusion on surfaces. *Advances in Physics* **51**(3), 949–1078 (2002)
- Albano, A.M., Bedeaux, D.: Non-equilibrium electrothermodynamics of polarizable multicomponent fluids with an interface. *Physica* **147A**, 407–435 (1987)
- Anderson, J.: Hypersonic and high temperature gas dynamics. McGraw Hill, New York NY (1989)
- Aris, R.: Vectors, tensors, and the basic equations of fluid mechanics. Dover publications, New York NY (1989)
- Balat, M., Czerniak, M., Badie, J.M.: Thermal and chemical approaches for oxygen catalytic recombination evaluation on ceramic materials at high temperature. *Applied Surface Science* **120**(3–4), 225–338 (1997)
- Balat-Pichelin, M., Badie, J.M., Berjoan, R., Boubert, P.: Recombination coefficient of atomic oxygen on ceramic materials under earth re-entry conditions by optical emission spectroscopy. *Chemical Physics* **291**(2), 181–194 (2003)
- Balat-Pichelin, M., Bêche, M.: Atomic oxygen recombination on the ODS PM 1000 at high temperature under air plasma. *Applied Surface Science* **256**(16), 4906–4914 (2010)
- Barbante, P., Chazot, O.: Flight extrapolation of plasma wind tunnel stagnation region flowfield. *Journal of Thermophysics and Heat Transfer* **20**(2), 493–499 (2006)
- Barbato, M., Giordano, D., Bruno, C.: Comparison between finite rate and other catalytic boundary conditions for hypersonic flows. In: 6th AIAA/ASME Joint Thermophysics and Heat Transfer Conference, June 20–23, Colorado Springs CO, AIAA 94–2074. American Institute of Aeronautics and Astronautics (1994)
- Barbato, M., Giordano, D., Muylaert, J., Bruno, C.: Comparison of catalytic wall conditions for hypersonic flows. *Journal of Spacecraft and Rockets* **33**(5), 620–627 (1996)
- Barrer, R.: Diffusion in and through solids. Cambridge University Press, London (1951)
- Bedeaux, D.: Nonequilibrium thermodynamics and statistical physics of surfaces. In: I. Prigogine, S.A. Rice (eds.) *Advances in Chemical Physics*, vol. LXIV, pp. 47–109. John Wiley and Sons, New York NY (1986)
- Bedeaux, D., Albano, A.M., Mazur, P.: Boundary conditions and non-equilibrium thermodynamics. *Physica* **82A**, 438–462 (1976)
- Bedra, L., Balat-Pichelin, M.: Comparative modeling study and experimental results of atomic oxygen recombination on silica-based surfaces at high temperature. *Aerospace Science and Technology* **9**(4), 318–328 (2005)
- Bellas-Chatzigeorgis, G., Barbante, P., Magin, T.: Development of detailed chemistry models for boundary layer catalytic recombination. In: Proceedings of the 8th European Symposium on Aerothermodynamics for Space Vehicles, 2–5 March, Lisbon, Portugal. European Space Agency (2015). URL <http://www.congrexprojects.com/Custom/15A01/Index.html>
- Bianchi, D.: Modeling of ablation phenomena in space applications. Ph.D. thesis, Dipartimento di Ingegneria Meccanica e Aerospaziale, Università di Roma (2007)
- Bianchi, D., Nasuti, F.: Carbon-carbon nozzle erosion and shape-change effects in full-scale solid-rocket. *Journal of Propulsion and Power* **28**(4), 820–830 (2012)
- Bianchi, D., Nasuti, F., Martelli, E.: Coupled analysis of flow and surface ablation in carbon-carbon rocket nozzles. *Journal of Spacecraft and Rockets* **46**(3), 492–500 (2009)
- Bianchi, D., Nasuti, F., Onofri, M.: Thermochemical erosion analysis for graphite/carbon-carbon rocket nozzles. *Journal of Spacecraft and Rockets* **27**(1), 197–205 (2011)
- Bianchi, D., Turchi, A., Nasuti, F.: Numerical analysis of nozzle flows with finite-rate surface ablation and pyrolysis-gas injection. In: 47th AIAA/ASME/SAE/ASEE Joint Propulsion Conference & Exhibit, 31 July–03 August, San Diego CA, AIAA 2011–6135. American Institute of Aeronautics and Astronautics (2011)
- Billing, G.D.: Dynamics of molecule surface interactions. John Wiley & Sons, New York NY (2000)
- Borman, V.D., Krylov, S.Y., Prosyantov, A.V.: Theory of nonequilibrium phenomena at a gas-solid interface. *Soviet Physics JETP* **67**(10), 2110–2121 (1988)
- Borman, V.D., Krylov, S.Y., Prosyantov, A.V.: Fundamental role of unbound surface particles in transport phenomena along a gas-solid interface. *Soviet Physics JETP* **70**(6), 1013–1022 (1990)
- Buff, F.P.: The theory of capillarity. In: S. Flügge (ed.) *Encyclopedia of Physics - Structure of Liquids*, vol. X, pp. 281–304. Springer, Berlin, Germany (1960)
- Cacciatore, M., Rutigliano, M., Billing, G.: Energy flows, recombination coefficients and dynamics for oxygen recombination on silica surfaces. In: 7th AIAA/ASME Joint Thermophysics and Heat Transfer Conference, June 15–18, Albuquerque NM, AIAA 98–2843. American Institute of Aeronautics and Astronautics (1998)
- Cacciatore, M., Rutigliano, M., Billing, G.: Eley-Rideal and Langmuir-Hinshelwood recombination coefficients for oxygen on silica surfaces. *Journal of Thermophysics and Heat Transfer* **13**(2), 566–571 (1999)
- Callen, H.: Thermodynamics. John Wiley & Sons, New York NY (1963). First publication in 1960
- Çengel, Y.A., Ghajar, A.J.: Heat and mass transfer, 5 edn. McGraw Hill, New York NY (2015)
- Cozmuta, I.: Molecular mechanisms of gas surface interactions in hypersonic flow. In: 39th AIAA Thermophysics Conference, June 25–28, Miami FL, AIAA 2007–4047. American Institute of Aeronautics and Astronautics (2007)
- Defay, R., Prigogine, I., Sanfeld, A.: Surface thermodynamics. *Journal of Colloid and Interface Science* **58**(3), 498–510 (1977)
- Dell’Isola, F., Kosinski, W.: Deduction of thermodynamic balance laws for bidimensional nonmaterial directed continua modelling interphase layers. *Archives of Mechanics* **45**(3), 333–359 (1993)
- Di Benedetto, S., Bruno, C.: Novel semi-empirical model for finite rate catalysis with application to PM1000 material. *Journal of Thermophysics and Heat Transfer* **24**(1), 50–59 (2010)
- Einstein, A.: Folgerungen aus den capillaritätsercheinungen. *Annalen der Physik* **4**(4), 513–523 (1901)
- Esser, B., Gülhan, A., Koch, U.: Experimental determination of recombination coefficients at high pressures. In: Proceedings of the 8th European Symposium on Aerothermodynamics for Space Vehicles, 2–5 March, Lisbon, Portugal. European Space Agency (2015). URL <http://www.congrexprojects.com/Custom/15A01/Index.html>
- Fang, G., Ward, C.A.: Temperature measured close to the interface of an evaporating liquid. *Physical Review E: Statistical, Nonlinear, and Soft Matter Physics* **59**(1), 417–428 (1999)

37. Fay, J.A., Riddell, F.R.: Theory of stagnation point heat transfer in dissociated air. *Journal of the Aeronautical Sciences* **25**(2), 73–85 (1958)
38. Fertig, M.: Finite rate surface catalysis modelling of PM1000 and SiC employing the DLR CFD solver TAU. In: Proceedings of the 8th European Symposium on Aerothermodynamics for Space Vehicles, 2-5 March, Lisbon, Portugal. European Space Agency (2015). URL <http://www.congrexprojects.com/Custom/15A01/Index.html>
39. Fick, A.: Ueber diffusion. *Annalen der Physik und Chemie* **94**(1), 59–86 (1855)
40. Finamore, F., Bruno, C.: Theoretical predictions of hydrogen recombination on zirconia. *Journal of Thermophysics and Heat Transfer* **21**(2), 267–275 (2007)
41. Gatignol, R., Prud'homme, R.: Mechanical and thermodynamical modeling of fluid interfaces. *Series on Advances in Mathematics for Applied Sciences*, vol. 58. World Scientific Publishing, Singapore (2001)
42. Gauss, C.F.: Principia generalia theoriae figurae fluidorum in statu aequilibrum. In: Werke, vol. V, 2 edn., pp. 29–77. Königlich Gesellschaft der Wissenschaften, Göttingen, Germany (1877). Originally presented as “Commentationes societatis regiae scientiarum Gottingensis recentiores, vol VII, Göttingae, MDCCCXXX”.
43. Gibbs, J.W.: On the equilibrium of heterogeneous substances. *Transactions of the Connecticut Academy* **3**, 108–248 (1876)
44. Gibbs, J.W.: On the equilibrium of heterogeneous substances. *Transactions of the Connecticut Academy* **3**, 343–524 (1878)
45. Gibbs, J.W.: On the equilibrium of heterogeneous substances (abstract). *American Journal of Science* **16**(3), 441–458 (1878). Abstract of the papers in the Transactions of the Connecticut Academy [43,44].
46. Gibbs, J.W.: The Scientific Papers - Thermodynamics, vol. 1. Longmans, Green and Co., London (1906)
47. Gibbs, J.W.: The Collected Works - Thermodynamics, vol. 1. Longmans, Green and Co., New York NY (1928)
48. Gogosov, V.V., Naletova, V.A., Bin, C.Z., Shaposhnikova, G.A.: Conservation laws for the mass, momentum, and energy on a phase interface for true and excess surface parameters. *Fluid Dynamics* **18**(6), 923–930 (1983)
49. Goodman, F., Wachman, H.: Dynamics of gas-surface scattering. Academic Press, New York NY (1976)
50. Goulard, R.: On catalytic recombination rate in hypersonic stagnation heat transfer. *Journal of Jet Propulsion* **28**(11), 737–745 (1958)
51. Groß, A.: Theoretical surface science, 2 edn. Springer, Berlin, Germany (2009)
52. Guggenheim, E.A.: The thermodynamics of interfaces in systems of several components. *Transactions of the Faraday Society* **35**, 397–412 (1940)
53. Gurtin, M.E., Weissmüller, J., Larché, F.: A general theory of curved deformable interfaces in solids at equilibrium. *Philosophical Magazine A* **78**(5), 1093–1109 (1998)
54. Herdrich, G., Fertig, M., Löhe, S., Pidan, S., Auweter-Kurtz, M., Laux, T.: Oxidation behavior of siliconcarbide-based materials by using new probe techniques. *Journal of Spacecraft and Rockets* **42**(5), 817–824 (2005)
55. Hetnarski, R., Eslami, M.R.: Thermal stresses - advanced theory and applications, *Solid Mechanics and its Applications*, vol. 158. Springer (2009)
56. Javili, A., Kaessmair, S., Steinmann, P.: General imperfect interfaces. *Computer Methods in Applied Mechanics and Engineering* **275**, 76–97 (2014)
57. Javili, A., McBride, A., Steinmann, P.: Thermomechanics of solids with lower-dimensional energetics: on the importance of surface, interface, and curve structures at the nanoscale. A unifying review. *Applied Mechanics Reviews* **65**, (010,802–) 1–31 (2013)
58. Joiner, N., Esser, B., Fertig, M., Gülhan and Georg Herdrich, A., Massuti-Ballester, B.: Development of an innovative validation strategy of gas-surface interactions modeling for re-entry applications. *CEAS Space Journal* **8**(4), 237–255 (2015)
59. Keenan, J.A., Candler, G.: Simulation of ablation in earth atmospheric entry. In: 28th AIAA Thermophysics Conference, July 6-9, Orlando FL, AIAA 93-2789. American Institute of Aeronautics and Astronautics (1993)
60. Keenan, J.A., Candler, G.: Simulation of graphite sublimation and oxidation under re-entry conditions. In: 6th AIAA/ASME Joint Thermophysics and Heat Transfer Conference, June 20-23, Colorado Springs CO, AIAA 94-2083. American Institute of Aeronautics and Astronautics (1994)
61. Kendall, R., Bartlett, E., Rindal, R., Moyer, C.: An analysis of the coupled chemically reactin boundary layer and charring ablator. Tech. Rep. NASA CR-1060, NASA (1968)
62. Kjelstrup, S., Bedeaux, D.: Non-equilibrium thermodynamics of heterogeneous systems, *Series on Advances in Statistical Mechanics*, vol. 16. World Scientific Publishing, Singapore (2008)
63. Knudsen, M.: Die molekulare wärmeleitung der gase und der akkommodationskoeffizient. *Annalen der Physik* **11**(4), 593–656 (1911)
64. Kolesnikov, A.: Concept of the local thermo-chemical simulation for re-entry problem: validation & applications. In: Proceedings of the Ninth Thermal and Fluids Analysis Workshop, August 31 - September 4, 1998, Cleveland OH, NASA/CP-1999-208695, pp. 107–116. Glenn Research Center, National Aeronautics and Space Administration (1999)
65. Kolesnikov, A.: Combined measurements and computations of high enthalpy and plasma flows for determination of TPM surface catalicity. In: Measurements techniques for high enthalpy and plasma flows, *RTO EN*, vol. 8, pp. 8A 1–16. NATO Research and Technology Organization, Neuilly-sur-Seine, France (2000). Von Kármán Institute for Fluid Dynamics Lecture Series, 25-29 October 1999, Rhode-Saint-Gènes, Belgium.
66. Kolesnikov, A.: Extrapolation from high enthalpy test to flight based on the concept of local heat transfer simulation. In: Measurements techniques for high enthalpy and plasma flows, *RTO EN*, vol. 8, pp. 8B 1–14. NATO Research and Technology Organization, Neuilly-sur-Seine, France (2000). Von Kármán Institute for Fluid Dynamics Lecture Series, 25-29 October 1999, Rhode-Saint-Gènes, Belgium.
67. Kolesnikov, A., Gordeev, A., Vasil'evskii, S.: Simulation of stagnation point heating and predicting surface catalicity for the EXPERT re-entry conditions. In: H. Lacoste, L. Ouwehand (eds.) Proceedings of the 6th European Symposium on Aerothermodynamics for Space Vehicles, 3-6 November 2008, Versailles, France, *ESA SP*, vol. 659, pp. 481–487. European Space Agency, Noordwijk, The Netherlands (2009)
68. Kolesnikov, A., Pershin, I., Vasil'evskii, S.: Predicting catalicity of Si-based coating and stagnation point heat transfer in high-enthalpy CO<sub>2</sub> subsonic flows for the Mars entry conditions. In: A. Wilson (ed.) Proceedings of the International Workshop on Planetary Probe Atmospheric Entry and Descent Trajectory Analysis and Science, 6-9 October 2003, Lisbon, Portugal, *ESA SP*, vol. 544, pp. 77–83. European Space Agency, Noordwijk, The Netherlands (2004)
69. Kolesnikov, A., Pershin, I., Vasil'evskii, S., Yakushin, M.: Study of quartz surface catalicity in dissociated carbon dioxide subsonic flows. *Journal of Spacecraft and Rockets* **37**(5), 573–579 (2000)
70. Kolesnikov, A., Yakushin, M., Pershin, I., Vasil'evskii, S.: Heat transfer simulation and surface catalicity prediction at the Martian atmosphere entry conditions. In: 9th International Space Planes and Hypersonic Systems and Technologies Conference, November 1-4, Norfolk VA, AIAA 99-4892. American Institute of Aeronautics and Astronautics (1999)

71. Kolesnikov, A., Yakushin, M., Pershin, I., Vasil'evskii, S., Chazot, O., Vancrayenest, B., Muylaert, J.: Comparative study of surface catalytic under subsonic air test conditions. In: R.A. Harris (ed.) Proceedings of the Fourth European Symposium on Aerothermodynamics for Space Vehicles, 15-18 October 2001, Capua, Italy, *ESA SP*, vol. 487, pp. 481–488. European Space Agency, Noordwijk, The Netherlands (2002)
72. Kolesnikov, A., Yakushin, M., Vasil'evskii, S., Pershin, I., Gordeev, A.: Catalysis heat effects on quartz surface in high-enthalpy subsonic oxygen & carbon dioxide flows. In: R.A. Harris (ed.) Proceedings of the Third European Symposium on Aerothermodynamics for Space Vehicles, 24-26 November, Noordwijk, The Netherlands, *ESA SP*, vol. 426, pp. 537–544. European Space Agency, Noordwijk, The Netherlands (1998)
73. Kovac, J.: Non-equilibrium thermodynamics of interfacial systems. *Physica* **86A**, 1–24 (1977)
74. Kovalev, V., Kolesnikov, A.: Experimental and theoretical simulation of heterogeneous catalysis in aerothermochemistry (a review). *Fluid Dynamics* **40**(5), 669–693 (2005)
75. Kovalev, V., Kolesnikov, A., Krupnov, A., Yakushin, M.: Analysis of phenomenological models describing the catalytic properties of high-temperature reusable coatings. *Fluid Dynamics* **21**(6), 910–919 (1996)
76. Krylov, S.Y., Beenakker, J.J.M., Tringides, M.C.: On the theory of surface diffusion: kinetic versus lattice gas approach. *Surface Science* **420**, 233–249 (1999)
77. Krylov, S.Y., Prosyantov, A.V., Beenakker, J.J.M.: One dimensional surface diffusion. ii. density dependence in a corrugated potential. *Journal of Chemical Physics* **107**(17), 6970–6979 (1997)
78. Langmuir, I.: Part II.—“Heterogeneous reactions”. Chemical reactions on surfaces. *Transactions of the Faraday Society* **17**, 607–620 (1922)
79. Laplace, P.S.: Sur l'action capillaire et supplément a la théorie de l'action capillaire. In: *Traité de Mécanique Céleste, Supplément au Livre X*, vol. IV, pp. 349–501. Courcier Imprimeur-Libraire, Paris, France (1805)
80. Lees, L.: Laminar heat transfer over blunt nosed bodies at hypersonic flight speeds. *Journal of Jet Propulsion* **26**(4), 259–269 (1956)
81. Levich, V.G., Krylov, V.S.: Surface-tension-driven phenomena. *Annual Review of Fluid Mechanics* **1**, 293–316 (1969)
82. Massuti-Ballester, B., Herdrich, G.: Gas-surface interaction. Experimental determination of PM1000 and CVD-C/SiC catalytic properties. In: Proceedings of the 8th European Symposium on Aerothermodynamics for Space Vehicles, 2-5 March, Lisbon, Portugal. European Space Agency (2015). URL <http://www.congrexprojects.com/Custom/15A01/Index.html>
83. Massuti-Ballester, B., Pidan, S., Herdrich, G., Fertig, M.: Recent catalysis measurements at IRS. *Advances in Space Research* **56**, 742–765 (2015)
84. Maxwell, J.C.: Capillary action. In: *The Scientific Papers*, vol. 2, chap. LXXXIII, pp. 541–591. Cambridge University Press, Cambridge UK (1890)
85. Mehrer, H.: Diffusion in solids, *Springer Series in Solid-State Physics*, vol. 155. Springer, Berlin, Germany (2007)
86. Milos, F., Rasky, D.: Review of numerical procedures for computational surface thermochemistry. *Journal of Thermophysics and Heat Transfer* **8**(1), 24–34 (1994)
87. Minkowski, H.: Kapillarität. In: A. Sommerfeld (ed.) *Encyclopädie der mathematischen wissenschaften, Physik*, vol. 5 (teil 1), chap. 9, pp. 558–613. Teubner, Leipzig, Germany (1903–1921). Issue 4 dated 25. IV. 1907.
88. Moradi, O.: Thermodynamics of interfaces. In: J.C. Moreno-Pirajan (ed.) *Thermodynamics - Interaction Studies - Solid, Liquids and Gases*, chap. 8, pp. 201–250. InTech (2011)
89. Muiño, R.D., Busnengo, H.F., (Eds.): Dynamics of gas-surface interactions, *Springer Series in Surface Sciences*, vol. 50. Springer, Berlin, Germany (2013)
90. Napolitano, L.: Decomposition of fluid-dynamics balance equations. *L'Aerotecnica Missili e Spazio* **56**(4), 183–194 (1977)
91. Napolitano, L.: Macroscopic modeling of the thermodynamics of interfaces. In: AIAA 16th Aerospace Sciences Meeting, January 16-18, Huntsville AL, AIAA 78-222. American Institute of Aeronautics and Astronautics (1978)
92. Napolitano, L.: Thermodynamics and dynamics of pure interfaces. *Acta Astronautica* **5**, 655–670 (1978)
93. Napolitano, L.: Thermodynamics and dynamics of surface phases. *Acta Astronautica* **6**(9), 1093–1112 (1979)
94. Nasuti, F., Barbato, M., Bruno, C.: Material-dependent catalytic recombination modeling for hypersonic flows. *Journal of Thermophysics and Heat Transfer* **10**(1), 131–136 (1996)
95. NATO Research and Technology Organization: Experiment, modeling and simulation of gas-surface interactions for reactive flows in hypersonic flights, no. 142 in RTO-EN-AVT (2007). Von Kármán Institute for Fluid Dynamics Lecture Series, 6-10 February 2006, Rhode-Saint-Gènes, Belgium.
96. Nedeá, S.V., Pathak, A., Giordano, D., Solano-López, P.: (2016). In preparation
97. Ono, S., Kondo, S.: Molecular theory of surface tension in liquids. In: S. Függe (ed.) *Encyclopedia of Physics - Structure of Liquids*, vol. X, pp. 135–280. Springer, Berlin, Germany (1960)
98. Öttinger, H.C., Bedeaux, D., Venerus, D.C.: Nonequilibrium thermodynamics of transport through moving interfaces with application to bubble growth and collapse. *Physical Review E: Statistical, Nonlinear, and Soft Matter Physics* **80**(021606), 1–16 (2009)
99. Padilla, J.F., Boyd, I.D.: Assessment of gas-surface interaction models for computation of rarefied hypersonic flow. *Journal of Thermophysics and Heat Transfer* **23**(1), 96–105 (2009)
100. Panerai, F., Chazot, O.: Characterization of gas/surface interactions for ceramic matrix composite in high enthalpy, low pressure air flows. *Materials Chemistry and Physics* **134**(2–3), 597–607 (2012)
101. Panerai, F., Chazot, O., Helber, B.: Gas/surface interaction study on ceramic matrix composite thermal protection system in VKI plasmas facility. In: 42nd AIAA Thermophysics Conference, June 27-30, Honolulu HI, AIAA 2011-3642. American Institute of Aeronautics and Astronautics (2011)
102. Panerai, F., Marschall, J., Thömel, J., Vandendael, O., Hubin, A., Chazot, O.: Air plasma-material interactions at the oxidized surface of the PM1000 nickel-chromium superalloy. *Applied Surface Science* **316**, 385–397 (2014)
103. Park, C.: Nonequilibrium hypersonic aerothermodynamics. John Wiley & Sons, New York NY (1990)
104. Pidan, S., Auweter-Kurtz, M., Herdrich, G., Fertig, M.: Recombination coefficients and spectral emissivity of silicon carbide-based thermal protection materials. *Journal of Thermophysics and Heat Transfer* **19**(4), 566–571 (2005)
105. Poincaré, H.: *Capillarité*. Carré Éditeur, Paris, France (1895)
106. Poisson, S.D.: *Nouvelle théorie de l'action capillaire*. Bachelier, Paris, France (1831)
107. Probst, R.F.: Methods of calculating the equilibrium laminar heat transfer rate at hypersonic flights. *Journal of Jet Propulsion* **26**(6), 497–499 (1956)
108. Prosperetti, A.: Boundary conditions at a liquid-vapor interface. *Meccanica* **14**(1), 34–47 (1979)
109. Prud'homme, R.: Equations du bilan de systèmes comprenant des interfaces. *Journal de Physique* **32**(C5), 62–63 (1971). Supplément n° 10.
110. Prud'homme, R., Dudeck, M.: Equations de bilan d'un milieu conducteur avec champ électromagnétique. Rapport 76-2, Laboratoire d'Aérodynamique du CNRS, 4 ter, Route des Gardes 92190 Meudon, France (1976)



111. Rutigliano, M., Cacciatore, M.: Recombination of oxygen atoms on silica surface: new and more accurate results. *Journal of Thermophysics and Heat Transfer* **30**(1), 247–250 (2016). Technical note.
112. Rutigliano, M., Zazza, C., Sanna, N., Pieretti, A., Mancini, G., Barone, V., Cacciatore, M.: Oxygen adsorption on  $\beta$ -cristobalite polymorph: ab initio modeling and semiclassical time-dependent dynamics. *Journal of Physical Chemistry A* **113**(52), 15,366–15,375 (2009)
113. Sagis, L.: Dynamic properties of interfaces in soft matter: experiments and theory. *Reviews of Modern Physics* **83**(4), 1367–1403 (2011)
114. Şakraker, I., Turchi, A., Chazot, O.: Hypersonic aerothermochemistry duplication in ground plasma facilities: a flight-to-ground approach. *Journal of Spacecraft and Rockets* **v**(n), 1–10 (2015). Article in advance.
115. Sanfeld, A.: Introduction to the thermodynamics of charged and polarized layers, *Monographs in Statistical Physics and Thermodynamics*, vol. 10. John Wiley & Sons, London (1968)
116. Schmidtman, B.: Test-case studies on numerical algorithms for a macroscopic theory of gas/surface interactions finalized to hypersonic re-entry flows. Project report, Von Karman Institute for Fluid Dynamics, VKI, Chaussée de Waterloo 72, 1640 Rhode Saint Genèse, Belgium (2013). Supervisor: D. Giordano.
117. Schüßler, M., Auweter-Kurtz, M., Herdrich, G., Lein, S.: Surface characterization of metallic and ceramic TPS-materials for reusable space vehicles. In: 57th International Astronautical Congress, 2-6 October, Valencia, Spain, IAC 06-C2.6.09. American Institute of Aeronautics and Astronautics (2006)
118. Scott, C.D.: Effects of nonequilibrium and wall catalysis on Shuttle heat transfer. *Journal of Spacecraft and Rockets* **22**(5), 489–499 (1985)
119. Scott, C.D.: Wall catalytic recombination and boundary conditions in nonequilibrium hypersonic flows — with applications. In: J. Bertin, J. Periaux, J. Ballmann (eds.) *Advances in Hypersonics - Modeling Hypersonics Flows*, vol. 2, pp. 176–250. Birkhäuser, Boston MA (1992)
120. Scriven, L.E.: Dynamics of a fluid interface. *Chemical Engineering Science* **12**, 98–108 (1960)
121. Sedov, L.I.: Introduction to the mechanics of a continuous medium. Addison-Wesley Series in Mechanics and Thermodynamics. Addison-Wesley, Reading MA (1965)
122. Sedov, L.I.: Foundations of the non-linear mechanics of continua, 1 edn. International Series of Monographs in Interdisciplinary and Advanced topics in Science and Engineering. Pergamon Press, Oxford UK (1966)
123. Sedov, L.I.: A course in continuum mechanics, vol. 1. Wolters-Noordhoff, Groningen NL (1971)
124. Sedov, L.I.: Mécanique des Milieux Continus, vol. 1. Éditions MIR, Moscou (1975). French translation. Russian publication in 1970 by Izdatel'stvo Nauka, Moscow.
125. Shewmon, P.: Diffusion in solids, 2 edn. The Minerals, Metals & Materials Series. Springer, Switzerland (2016)
126. Slattery, J.C.: Surfaces I - Momentum and moment-of-momentum balances for moving surfaces. *Chemical Engineering Science* **19**(6), 379–385 (1964)
127. Slattery, J.C.: General balance equation for a phase interface. *Industrial & Engineering Chemistry Fundamentals* **6**(1), 108–115 (1967)
128. Slattery, J.C., Sagis, L., Oh, E.S.: Interfacial transport phenomena, 2 edn. Springer (2007)
129. Somorjai, G.: Introduction to surface chemistry and catalysis, 1 edn. John Wiley & Sons, New York NY (1994)
130. Somorjai, G.A., Li, Y.: Impact of surface chemistry. *Proceedings of the National Academy of Sciences of the United States of America* **108**(3), 917–924 (2011)
131. Thoemel, J., Chazot, O., Barbante, P.: Aspects of advanced catalysis modeling for hypersonic flows. In: *Proceedings of the Summer Program of the Center for Turbulence Research*, Stanford CA, pp. 29–41. Stanford University (2008)
132. Turchi, A.: A gas-surface interaction model for the numerical study of rocket nozzle flows over pyrolyzing ablative materials. Ph.D. thesis, Dipartimento di Ingegneria Meccanica e Aerospaziale, Università di Roma (2013)
133. Viviani, A.: State of the art of gas-surface interaction in hypersonic reentry flows. TRP *Development of a rigorous macroscopic theory of gas-surface interactions in hypersonic reentry flows*, contract 17387 TN-1, European Space Agency, ESTEC, Keplerlaan 1 2201 AZ Noordwijk, The Netherlands (2008)
134. Viviani, A., Pezzella, G.: Influence of surface catalicity on reentry aerothermodynamics and heat shield. In: 39th AIAA Thermophysics Conference, June 25-28, Miami FL, AIAA 2007-4047. American Institute of Aeronautics and Astronautics (2007)
135. Waals, J.D.v.d.: Théorie thermodynamique de la capillarité, dans l'hypothèse d'une variation continue de densité. *Archives Néerlandaises des Sciences Exactes et Naturelles* **28**, 121–209 (1895)
136. Waldmann, L.: Non-equilibrium thermodynamics of boundary conditions. *Zeitschrift für Naturforschung* **22a**, 1269–1280 (1967)
137. Wolf, C.: Vom einfluss der temperatur auf die erscheinungen in haarröhrchen. *Annalen der Physik und Chemie* **101**, 550–576 (1857)
138. Young, T.: An essay on the cohesion of fluids. *Philosophical Transactions of the Royal Society of London* **95**, 65–87 (1805)
139. Zangwill, A.: *Physics at surfaces*. Cambridge University Press, Cambridge, UK (1988)
140. Zazza, C., Rutigliano, M., Sanna, N., Barone, V., Cacciatore, M.: Oxygen adsorption on  $\beta$ -quartz model surfaces: some insights from density functional theory calculations and semi-classical time-dependent dynamics. *Journal of Physical Chemistry A* **116**(9), 1975–1973 (2012)